

AERO. & ASTRO. LIBRARY



**NATIONAL ADVISORY COMMITTEE  
FOR AERONAUTICS**

**REPORT 1170**

*Copy # 3*

**BEHAVIOR OF MATERIALS UNDER CONDITIONS  
OF THERMAL STRESS**

By S. S. MANSON



**1954**

For sale by the Superintendent of Documents, U. S. Government Printing Office, Washington 25, D. C. Yearly subscription, \$10; foreign, \$11.25;  
single copy price varies according to size ----- Price 35 cents



---

---

# **REPORT 1170**

---

## **BEHAVIOR OF MATERIALS UNDER CONDITIONS OF THERMAL STRESS**

By S. S. MANSON

Lewis Flight Propulsion Laboratory  
Cleveland, Ohio

---

---

# National Advisory Committee for Aeronautics

*Headquarters, 1512 H Street NW., Washington 25, D. C.*

Created by act of Congress approved March 3, 1915, for the supervision and direction of the scientific study of the problems of flight (U. S. Code, title 50, sec. 151). Its membership was increased from 12 to 15 by act approved March 2, 1929, and to 17 by act approved May 25, 1948. The members are appointed by the President, and serve as such without compensation.

JEROME C. HUNSAKER, Sc. D., Massachusetts Institute of Technology, *Chairman*

DETLEV W. BRONK, Ph. D., President, Rockefeller Institute for Medical Research, *Vice Chairman*

JOSEPH P. ADAMS, LL. D., member, Civil Aeronautics Board.  
ALLEN V. ASTIN, Ph. D., Director, National Bureau of Standards.  
PRESTON R. BASSETT, M. A., President, Sperry Gyroscope Co., Inc.  
LEONARD CARMICHAEL, Ph. D., Secretary, Smithsonian Institution.  
RALPH S. DAMON, D. Eng., President, Trans World Airlines, Inc.  
JAMES H. DOOLITTLE, Sc. D., Vice President, Shell Oil Co.  
LLOYD HARRISON, Rear Admiral, United States Navy, Deputy and Assistant Chief of the Bureau of Aeronautics.  
RONALD M. HAZEN, B. S., Director of Engineering, Allison Division, General Motors Corp.

RALPH A. OFSTIE, Vice Admiral, United States Navy, Deputy Chief of Naval Operations (Air).  
DONALD L. PUTT, Lieutenant General, United States Air Force, Deputy Chief of Staff (Development).  
DONALD A. QUARLES, D. Eng., Assistant Secretary of Defense (Research and Development).  
ARTHUR E. RAYMOND, Sc. D., Vice President—Engineering, Douglas Aircraft Co., Inc.  
FRANCIS W. REICHELDERFER, Sc. D., Chief, United States Weather Bureau.  
OSWALD RYAN, LL. D., member, Civil Aeronautics Board.  
Nathan F. TWINING, General, United States Air Force, Chief of Staff.

---

HUGH L. DRYDEN, Ph. D., *Director*

JOHN F. VICTORY, LL. D., *Executive Secretary*

JOHN W. CROWLEY, JR., B. S., *Associate Director for Research*

EDWARD H. CHAMBERLIN, *Executive Officer*

---

HENRY J. E. REID, D. Eng., Director, Langley Aeronautical Laboratory, Langley Field, Va.

SMITH J. DEFANCE, D. Eng., Director, Ames Aeronautical Laboratory, Moffett Field, Calif.

EDWARD R. SHARP, Sc. D., Director, Lewis Flight Propulsion Laboratory, Cleveland Airport, Cleveland, Ohio

---

LANGLEY AERONAUTICAL LABORATORY  
Langley Field, Va.

AMES AERONAUTICAL LABORATORY  
Moffett Field, Calif.

LEWIS FLIGHT PROPULSION LABORATORY  
Cleveland Airport, Cleveland, Ohio

*Conduct, under unified control, for all agencies, of scientific research on the fundamental problems of flight*



## REPORT 1170

### BEHAVIOR OF MATERIALS UNDER CONDITIONS OF THERMAL STRESS<sup>1</sup>

By S. S. MANSON

#### SUMMARY

*A review is presented of available information on the behavior of brittle and ductile materials under conditions of thermal stress and thermal shock. For brittle materials, a simple formula relating physical properties to thermal-shock resistance is derived and used to determine the relative significance of two indices currently in use for rating materials. The importance of simulating operating conditions in thermal-shock testing is deduced from the formula and is experimentally illustrated by showing that BeO could be either inferior or superior to  $Al_2O_3$  in thermal shock, depending on the testing conditions. For ductile materials, thermal-shock resistance depends upon the complex interrelation among several metallurgical variables which seriously affect strength and ductility. These variables are briefly discussed and illustrated from literature sources. The importance of simulating operating conditions in tests for rating ductile materials is especially to be emphasized because of the importance of testing conditions in metallurgy. A number of practical methods that have been used to minimize the deleterious effects of thermal stress and thermal shock are outlined.*

#### INTRODUCTION

When a material is subjected to a temperature gradient or when a composite material consisting of two or more materials having different coefficients of expansion is heated either uniformly or nonuniformly, the various fibers tend to expand different amounts in accord with their individual temperatures and temperature coefficients of expansion. To enable the body to remain continuous, rather than allowing each fiber to expand individually, a system of thermal strain and associated stresses may be introduced depending upon the shape of the body and the temperature distribution. If the material cannot withstand the stresses and strains, rupture may occur.

Brittle and ductile materials react in considerably different manners to thermal stress. Brittle materials can endure only a very small amount of strain before rupture; ductile materials can undergo appreciable strain without rupture. Since thermal stress behavior depends essentially on the ability of the material to absorb the induced strains necessary to maintain a continuous body upon the application of a thermal gradient, brittle materials cannot readily withstand

these superimposed strains without inducing enough stress to cause rupture; ductile materials, on the other hand, can usually withstand these additional strains, but may ultimately fail if subjected to a number of cycles of imposed temperature.

The problem of thermal stress is of great importance in current high-power engines. The present trend toward increasing temperatures has necessitated the use of refractory materials capable of withstanding much higher temperatures than normal engineering materials. One salient property of these materials is lack of ductility. For this reason, thermal stress is one of the most important design criteria in the application of these materials. Thermal stress is also currently receiving considerable attention in connection with ductile materials since there is considerable evidence that failure of many ductile engine components can be attributed to thermal cycling. The problem of high-speed flight, with attendant increases of temperature and temperature gradients in aircraft bodies, has further generated concern over the significance of thermal stress in ductile materials.

Thermal stress and thermal shock may be distinguished by the fact that in thermal shock the thermal stresses are produced by transient temperature gradients, usually sudden ones. For example, if a body originally at one uniform temperature is suddenly immersed in a medium of different temperature, a condition of thermal shock is introduced. At any instant the stresses are determined by the temperature distribution and are no different from what they would be if this temperature distribution could be obtained in the steady-state condition. But the temperature gradients that can be established in the transient state are generally much higher than those that occur in the steady state, and hence thermal shock is important relative to ordinary thermal stress because of the higher stress that can be induced. Another distinction between thermal stress and thermal shock is that in thermal shock the rate of application of stress is very rapid, and many materials are affected by the rate at which load is applied. Some materials are embrittled by rapid application of stress and therefore may not be able to withstand a thermal shock stress which if applied slowly could readily be absorbed.

<sup>1</sup> Supersedes NACA TN 2933, "Behavior of Materials Under Conditions of Thermal Stress" by S. S. Manson, 1953. Based on lecture presented at Symposium on Heat Transfer, University of Michigan, June 27-28, 1952.



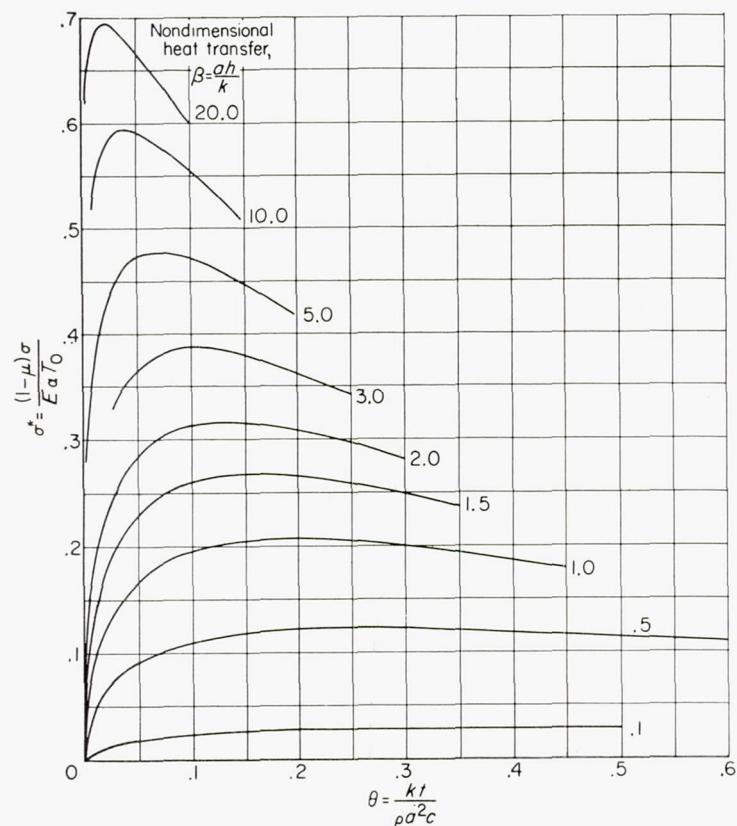


FIGURE 1.—Nondimensional stress versus nondimensional time for surface of flat plate.

It is also necessary to distinguish between a single cycle of thermal stress and thermal fatigue. When failure is caused by the application of several similar thermal stress cycles, rather than a single cycle, the process is referred to as thermal fatigue. The processes that take place in a body in successive cycles of stress application are extremely complex; the mechanism leading to cyclic failure is as yet incompletely understood. In most of the basic work, therefore, attention is directed at the conditions under which failure will occur in one cycle merely because this case lends itself to analysis. The problem of thermal fatigue is, of course, a most important one in engineering application.

The objectives of this presentation are: First, some of the information contained in recent publications on the mathematics of thermal shock will be outlined, and a simple formula will be derived for correlation of thermal shock behavior with material properties. Second, the variables in the simplified relation will be examined and from it methods for minimizing thermal stress will be deduced. For brittle materials the single-cycle criterion of failure will be considered; for ductile materials the discussion will be directed at available information on the problem of thermal fatigue.

#### THERMAL SHOCK OF BRITTLE MATERIALS AS DEDUCED FROM STUDY OF FLAT PLATE

**General equation for stress.**—In order to make the discussion specific, the case considered is that of a homogeneous

flat plate initially at uniform temperature and suddenly immersed in a medium of lower temperature. This case is treated because the temperature problem of the flat plate is well known, and because most of the recent publications on the thermal stress problem also consider this case (for example, refs. 1 and 2). There is, therefore, a considerable background of information from which to draw results and with which to make comparisons. Furthermore, most of the one-dimensional problems can be treated in essentially the same way as the flat plate problem treated herein, and therefore any important conclusions that pertain to the flat plate are probably also valid for other shapes, provided that the necessary changes are made in the constants. Note also that in this case the temperature problem is one-dimensional; that is, in the flat plate, temperature variations will be considered only in the thickness direction. The problem is treated in this way because there are relatively few two-dimensional problems solved in the literature and also because the qualitative conclusions reached in the flat plate problem are believed to apply to more complicated cases.

The first problem in connection with the flat plate is to determine the temperature distribution at a time  $t$  after the surrounding temperature has been changed. Once this temperature has been determined, the stresses can readily be determined in accordance with very simple formulas derived from the theory of elasticity. Assuming that the properties of the material do not vary with temperature and that the material is elastic, the following equation can be written for the stress at any point in the thickness of the plate:

$$\sigma^* = \frac{T_{av} - T}{T_0} \quad (1)$$

Physically,  $\sigma^*$  can be considered as the ratio of the stress actually developed to the stress that would be developed if thermal expansion were completely constrained. The formula for  $\sigma^*$  is

$$\sigma^* = \frac{\sigma(1-\mu)}{E\alpha T_0} \quad (2)$$

where

- $\sigma$  actual stress
- $\mu$  Poisson's ratio
- $E$  elastic modulus
- $\alpha$  coefficient of expansion
- $T_{av}$  average temperature across thickness of plate
- $T$  temperature at point where stress is considered
- $T_0$  initial uniform temperature of plate above ambient temperature (ambient temperature assumed to be zero for simplicity)

**Stress at surface.**—In order to obtain the surface stress, it is therefore necessary first to determine the average temperature and the surface temperature. The temperature problem has been thoroughly treated in the literature and the result is usually given in the form of an infinite series. In figure 1 are shown the results of some computations that have been made by substituting the exact series solution for temperature into the stress equations.



In the exact solution there are three important variables. First is the reduced stress, already mentioned, and second, the value  $\beta$  which is equal to  $\frac{ah}{k}$  (where  $a$  is the half thickness of the plate,  $h$  is the heat-transfer coefficient, and  $k$  is the conductivity of the material). The heat-transfer coefficient is defined as the amount of heat transferred from a unit area of the surface of the plate per unit temperature difference between the surface and the surrounding medium. The variables  $a$ ,  $h$ , and  $k$  always occur as a group as a result of the manner in which they appear in the differential equation; therefore, in the generalized treatment of the problem it is not the individual value of  $a$ ,  $h$ , or  $k$  that is of importance but their value as grouped together to form the term  $\beta$ . The term  $\beta$  is generally known as Biot's modulus, but in the present discussion it will be called the nondimensional heat-transfer parameter. The third important variable is  $\theta$ , which will be called nondimensional time. As shown,  $\theta = \frac{kt}{\rho ca^2}$  where  $k$  is again the conductivity,  $t$  is the time,  $a$  is the half thickness,  $\rho$  is the density of the material, and  $c$  is the specific heat. In this figure the nondimensional stress at the surface has been plotted as a function of nondimensional time for various examined values of nondimensional heat transfer. This plot contains the essentials of the entire solution of surface stress in the flat plate problem; the attainment of further relations of interest is just a matter of replotting.

**Maximum stress at surface.**—It is of interest to consider the maximum surface stress as a function of  $\beta$ . In references 1 and 2 the maximum stress is analytically determined by suitable approximations of the series solution. For example, Bradshaw (ref. 1) considers only small values of  $\beta$ , for which all but the first two terms of the series may be omitted. The maximum stress is then obtained by setting the derivative of stress with time equal to zero. Accurate results are thus obtained, but they are valid only for small values of  $\beta$ . Since figure 1 gives the complete variation of stress with time, it is not necessary to differentiate; the maximum value of stress may be read directly from the curve for each value of  $\beta$ , and the results will be correct over the complete range of  $\beta$  rather than only in certain intervals. A plot of  $\sigma^*_{max}$  versus  $\beta$  is shown in figure 2. From this curve it is seen that the variation of nondimensional maximum stress with  $\beta$  is roughly linear for small values of  $\beta$  but becomes asymptotic to a value of unity at very large values of  $\beta$ .

In order to obtain a simple formula for the curve of figure 2, an approach first used by Buessem (ref. 3) will be used; but by somewhat more general assumptions, a more accurate formula will be obtained. This derivation is obtained with the use of figure 3. In this figure the center line represents the center of the plate; the two solid vertical lines represent the surfaces of the plate. Ordinates measure temperatures. The temperature distributions through the thickness of the plate at several different times  $t_0$ ,  $t_1$ ,  $t_2$ ,  $t_3$  after the sudden application of cold atmosphere are shown by the curves

PQ, P'Q', etc. These curves must fit two boundary conditions: (1) At the center they must have a horizontal tangent because the center of the plate is a line of symmetry, and no heat is transferred across the center line; (2) at the surface the slope must be in accord with the surface heat-transfer coefficient, which is equivalent to the condition that the tangent to the curves at the surface pass through the fixed point O representing the ambient temperature which has been taken equal to zero. These temperature distributions must also satisfy the differential equations of heat transfer, which is achieved by adjusting certain constants so that the final result will be consistent with the curve of figure 2, which of course does satisfy the differential equation.

It is assumed that the temperature curve can be fitted by an equation of the form

$$T = T_{2,c} - M \left( \frac{x}{a} \right)^n \quad (3)$$

where

$T_{2,c}$  temperature at center of plate at time when stress at surface is a maximum, as yet undetermined

$M, n$  constants to be best determined to fit theoretical results

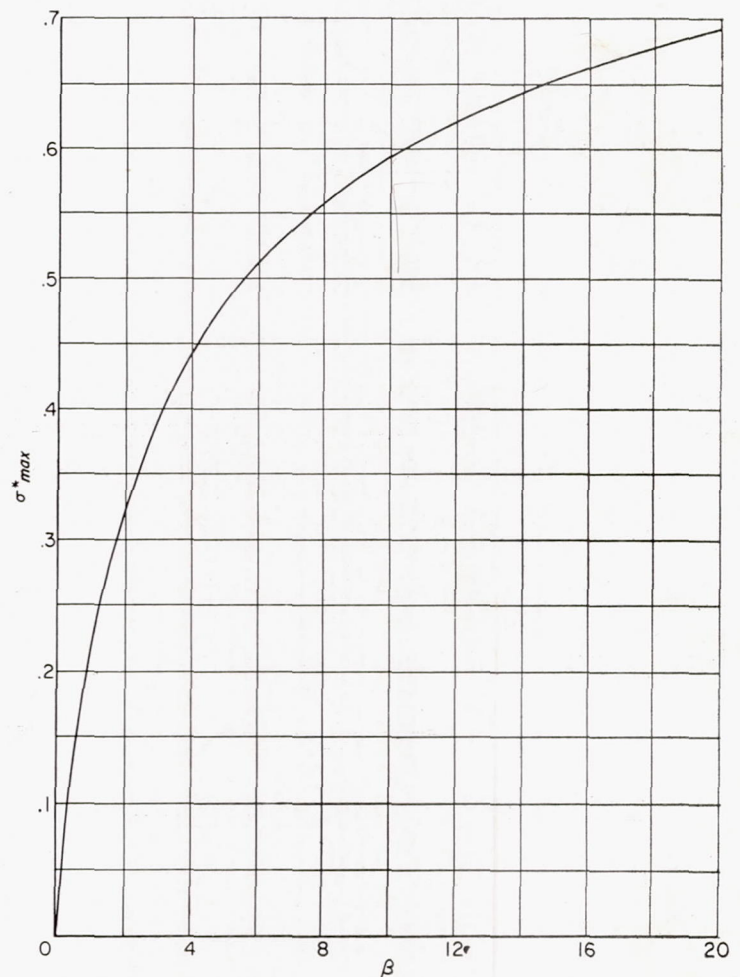
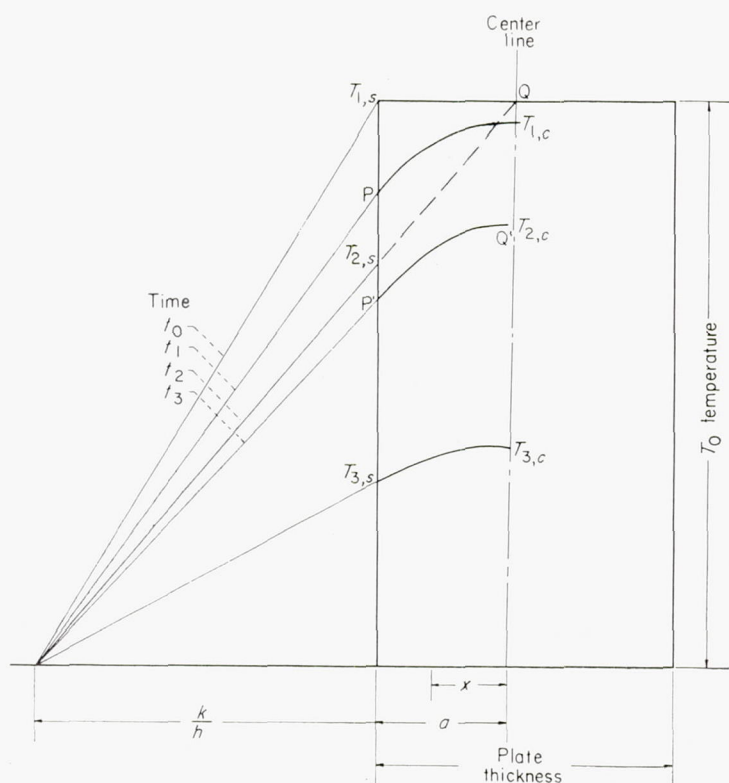


FIGURE 2.—Analytical solution of nondimensional maximum stress versus nondimensional heat transfer.





$$T = T_{2,c} - M \left( \frac{x}{a} \right)^n$$

$$M = \frac{\beta T_{2,c}}{\beta + n} \quad (\text{surface boundary condition})$$

$$\sigma^* = \frac{T_{2,c}}{T_0} \cdot \frac{n}{n+1} \cdot \frac{\beta}{\beta+n} = \frac{R\beta}{\beta+n}$$

$$\frac{1}{\sigma^*} = \frac{1}{R} + \frac{n}{R} \cdot \frac{1}{\beta}$$

$$\sigma^* = \frac{\beta}{4+\beta} \quad (\text{Buessem, ref. 3})$$

FIGURE 3.—Formula for maximum stress at surface of plate (from ref. 3)

As long as  $n > 1$ , this equation will automatically satisfy the first boundary condition of horizontal tangency at  $x=0$ . If the surface condition  $-k \left( \frac{dT}{dx} \right)_a = h T_{2,s}$  is to be satisfied, the condition of equation (4) must be satisfied

$$M = \frac{\beta T_{2,c}}{\beta + n} \quad (4)$$

From equations (1), (3), and (4),

$$\sigma^*_{max} = \frac{T_{2,c}}{T_0} \cdot \frac{n}{n+1} \cdot \frac{\beta}{\beta+n} \quad (5)$$

or, if  $R = \frac{n T_{2,c}}{T_0(n+1)}$ , equation (5) readily reduces to

$$\frac{1}{\sigma^*_{max}} = \frac{1}{R} + \frac{n}{R} \cdot \frac{1}{\beta} \quad (6)$$

Equation (6) suggests that a plot of  $\frac{1}{\sigma^*_{max}}$  against  $\frac{1}{\beta}$  should be a straight line. When values of  $\sigma^*_{max}$  and  $\beta$  from figure 2

are used, the plot  $\frac{1}{\sigma^*_{max}}$  against  $\frac{1}{\beta}$  in figure 4 is obtained. It is seen that for  $\frac{1}{\beta} > 0.2$  or  $\beta < 5$ , a very good straight line can be fitted to the curve; the equation of this line is given by

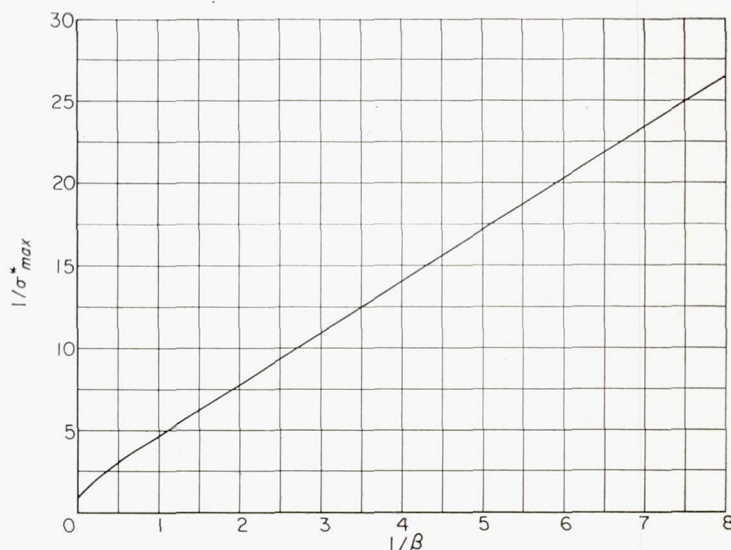
$$\frac{1}{\sigma^*_{max}} = 1.5 + \frac{3.25}{\beta} \quad \text{for } \beta < 5 \quad (7)$$

In the region  $1/\beta < 0.2$  (i. e.,  $\beta > 5$ ), the curve deviates somewhat from the straight line, curving downward and reaching a limit  $\sigma^* = 1.0$  at  $1/\beta = 0$  instead of a value of 1.5 predicted by the straight line. To make the formula accurate over the entire range, it is desirable to add a term that will be effective only in the very low range of  $1/\beta$  and cause the expression to reach the proper limit at  $1/\beta = 0$ . An exponential term serves this purpose well over the entire range of  $\beta$ ; therefore, the following equation relates  $\beta$  and  $\sigma^*$ :

$$\frac{1}{\sigma^*_{max}} = 1.5 + \frac{3.25}{\beta} - 0.5 e^{-16/\beta} \quad (8)$$

Figure 5 shows the correctness of fit of equation (8) and the exact results over the range  $0 < \beta < 20$ . For values of  $\beta$  between 0 and 5, the exponential term is negligible and the fit of the exact results with equation (7) is essentially the same as the fit with equation (8). No refined calculations have been carried out for values of  $\beta$  above 20, but a comparison of equation (8) with an asymptotic formula given by Cheng (ref. 2) indicates that equation (8) may be in error by as much as 5 percent at a value of  $\beta = 200$ . However, since most practical problems involve values of  $\beta$  below 20, equation (8) is seen to give results of unusually good accuracy over the practical range of  $\beta$ . If, however, greater accuracy is desired in the range of  $\beta$  from 5 to 20, the formula

$$\frac{1}{\sigma^*_{max}} = 1.0 + \frac{3.25}{\beta^{2/3}} \quad (8a)$$

FIGURE 4.—Relation between  $1/\beta$  and  $1/\sigma^*_{max}$ .



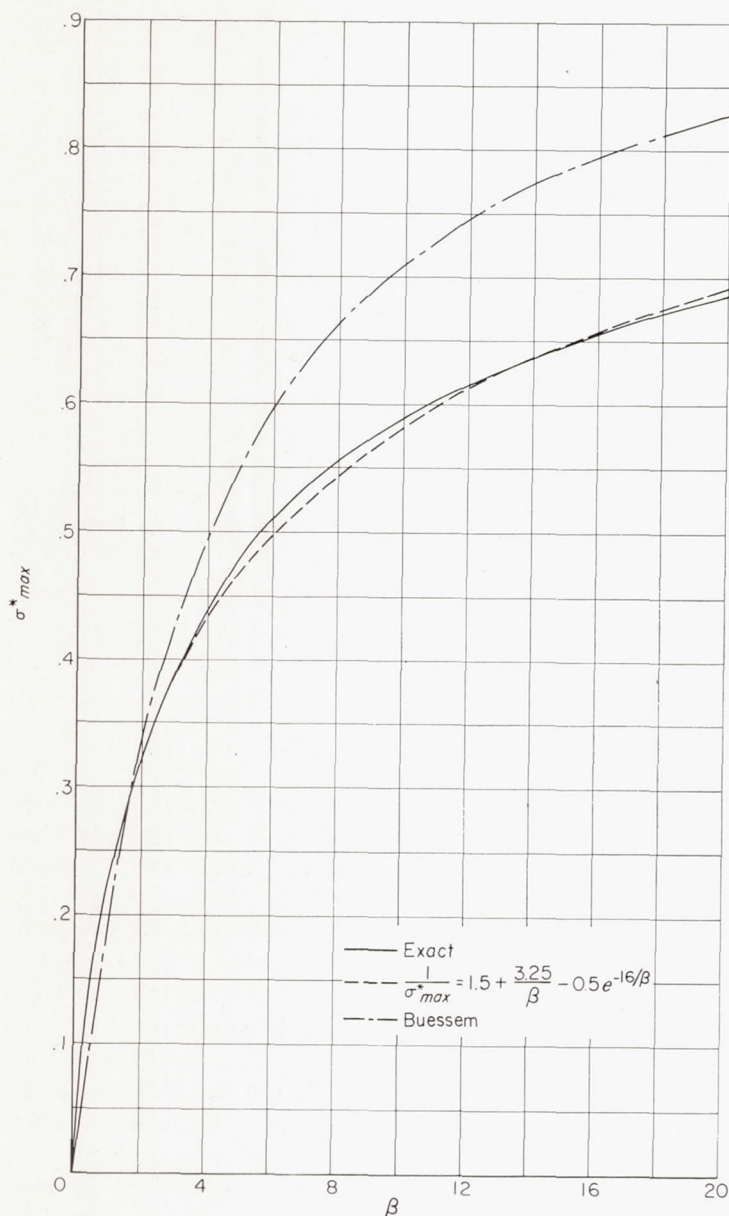


FIGURE 5.—Correlation of approximate formulas with exact solution for maximum stress.

can be used in this range together with equation (7) in the range  $0 < \beta < 5$ . Equation (8) has, however, the advantage of representing the entire range of  $\beta$  with a single formula.

In his original paper (ref. 3) Buessem derived a simplified formula for this case in another manner. It was assumed that the stress could be approximated by taking the temperature distribution in the plate at the time of maximum stress as the straight line PQ in figure 3. Determining first the surface stress for this temperature distribution and then adjusting the resultant formula so that it was consistent with the correct surface stress values at two values of  $\beta$  gave the following equation:

$$\frac{1}{\sigma_{max}^*} = 1 + \frac{4}{\beta} \quad (9)$$

Equation (9) is very similar in form to equation (7), but it does not fit the correct curve of  $\sigma^*$  against  $\beta$  quite so well as equation (8) over the entire range of  $\beta$ . Figure 5 shows the degree of correlation between analytical results of figure 2 and the simple formulas given in equations (7) and (8). Also shown is the correlation obtained with the Buessem formula, which, although very good, is not so close as that with the formulas presented herein.

**Thermal shock parameters.**—Use can now be made of the approximate formulas to correlate the maximum stress developed in a material with the physical properties of materials. In most cases, the value of  $\beta$  for reasonable heat-transfer coefficients, plate thicknesses, and conductivities is relatively low, so that the term 1.5 in equation (7) can be neglected compared with the value  $3.25/\beta$  for practical purposes. In this case, equation (7) becomes equation (10), which can be rewritten as equation (11).

$$\frac{1}{\sigma_{max}^*} = \frac{3.25}{\beta} \quad (10)$$

or

$$T_0 = \frac{k \sigma_{max}}{E \alpha} \cdot \frac{3.25 (1 - \mu)}{a h} \quad (11)$$

When failure occurs,  $\sigma_{max} = \sigma_b$  = breaking stress; hence,

$$T_{0, max} = \frac{k \sigma_b}{E \alpha} \cdot \frac{3.25 (1 - \mu)}{a h} \quad (11a)$$

This equation states that for a flat plate of thickness  $a$  and heat-transfer coefficient  $h$ , the maximum shock temperature that can be withstood by the plate is proportional to the product  $k \sigma_b / E \alpha$ . Since Poisson's ratio  $\mu$  is very similar for all materials, it is placed in the group of terms not involving material properties. This grouping  $k \sigma_b / E \alpha$  is identified as the thermal shock parameter used by Bobrowsky (ref. 4) and by others. Equation (11) gives a numerical measure of shock temperature that will cause failure and provides the basis for an index for listing materials in order of merit. Table I shows results of tests conducted in reference 4 showing the order of merit of several materials according to the thermal shock parameter  $k \sigma_b / E \alpha$ . These tests consisted of subjecting a round specimen 2 inches in diameter and  $1/4$  inch thick to thermal shock cycles until failure occurred. In this cycle the specimen was first heated to furnace temperature and then quenched in a stream of cold air directed parallel to the faces of this specimen. If the specimen survived 25 cycles at one furnace temperature, the furnace temperature was increased  $200^\circ$  F and the tests were repeated. In this way the temperature was raised until failure finally occurred. The table shows that a good correlation was obtained between the maximum temperature achieved and the thermal shock parameter  $k \sigma_b / E \alpha$ .

When equation (8) is again considered, it is seen that for very large values of  $\beta$  the value  $3.25/\beta$  can be neglected compared with the other terms and  $\sigma_{max}^*$  becomes equal



to unity. It is interesting to examine the meaning of  $\sigma_{max}^*=1$  and to determine under which conditions  $\sigma_{max}^*=1$  is achieved. The condition of  $\sigma_{max}^*=1$  means that

$$\sigma_{max} = \frac{E\alpha T_0}{1-\mu} \quad (12)$$

The product  $\alpha T_0$  is the contraction in the material that would take place if the temperature were reduced by  $T_0$  and the material allowed to contract freely. If contraction is completely prevented by application of stress, then  $\alpha T_0$  is the elastic strain that must be induced in the material to prevent this contraction, and this strain multiplied by the elastic modulus becomes the stress that must be applied. The term  $(1-\mu)$  results from the fact that the problem is for an infinite plate in which equal stresses are applied in two mutually perpendicular directions. In this case  $E\alpha T_0/(1-\mu)$  is the stress that must be applied in two perpendicular directions to completely prevent any contraction in the material. Hence, for very large values of  $ah/k$ , equation (8) states that the stress developed is just enough to prevent any thermal expansion. To obtain an index of merit for rating materials under the conditions of very large  $\beta$ , equation (12) is rewritten as equation (13), which suggests that this index is now  $\sigma_b/E\alpha$ ; and it is seen that the conductivity factor has vanished compared with the index  $k\sigma_b/E\alpha$ .

$$T_{0, max} = \frac{\sigma_b}{E\alpha} (1-\mu) \quad (13)$$

The implication is that the value of the conductivity of the material does not matter; the temperature that can be withstood is in proportion to  $\sigma_b/E\alpha$ . Physically, this result can be understood by examining the meaning of very large  $\beta$ , which condition can occur either if  $a$  is very large, if  $h$  is very large, or if  $k$  is very small. If  $a$  is very large, it means that the test body is very large and that the surface layers can be brought down to the temperature of the surrounding medium before any temperature change occurs in the bulk of the body. The surface layers cannot contract because to do so they would have to deform the remainder of the body, and this cannot be achieved for a very large body. Hence, in this case, complete constraint of contraction is imposed, and the stress developed is  $E\alpha T_0/(1-\mu)$  irrespective of the actual value of conductivity. Similarly, for large heat-transfer coefficients  $h$ , the same result can be expected. The surface is brought down to the temperature of the surrounding medium before the remainder of the body has had the time to respond to the imposed temperature difference. Hence, again complete constraint of contraction is imposed, and the stress developed is independent of conductivity. Finally, if the conductivity is very small, again only the surface layers can realize the imposed thermal shock conditions, the remainder of the body remaining essentially at the initial temperature. Again, complete constraint against thermal contraction is imposed and the stress is independent of the precise value of  $k$ , provided it is very small.

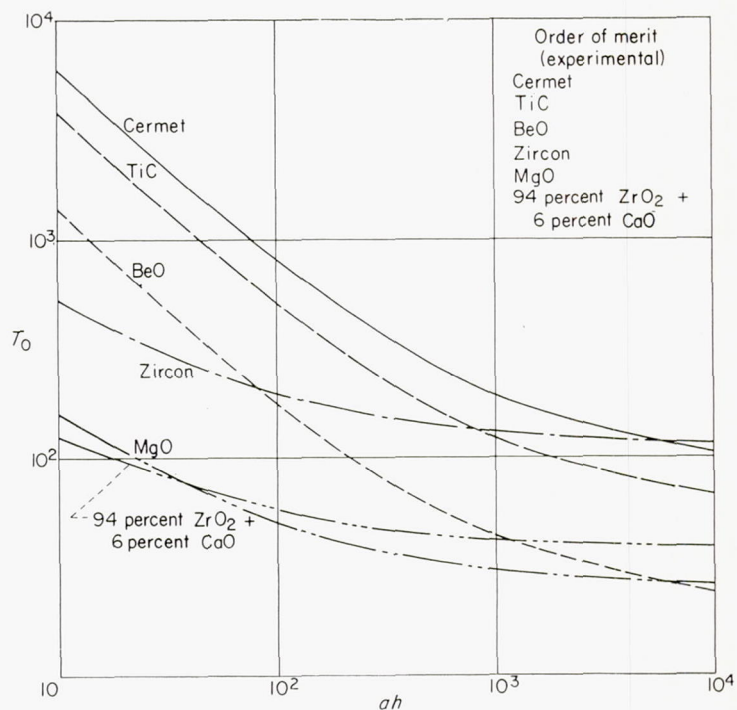


FIGURE 6.—Index of merit for different shock conditions.

That there are two thermal shock parameters at the two extremes of the  $\beta$  scale,  $k\sigma_b/E\alpha$  and  $\sigma_b/E\alpha$ , has recently been emphasized by Bradshaw (ref. 5). That both thermal shock parameters are necessary to determine completely the thermal shock resistance of a material has been emphasized by Buessem. The merit of equation (8) is that it provides a simple formula for determining the relative roles of the two parameters over the complete range of  $\beta$ .

**Significance of test conditions.**—The previous result, namely, that the index of merit is proportional to  $k\sigma_b/E\alpha$  for low values of  $\beta$  and proportional to  $\sigma_b/E\alpha$  for high values of  $\beta$ , suggests the importance of the test conditions used to evaluate materials. In figure 6 there is plotted the temperature that could be withstood in the test specimens described in reference 4, and shown in table I, for different values of  $ah$ , that is, if specimen thicknesses or heat-transfer coefficients had differed from the values actually used. These curves were obtained from equation (8) in conjunction with the material properties given in table I. It is seen that at the low values of  $ah$ , the test condition actually used being represented at a value of  $ah \approx 10$ , the order of merit of the materials, that is, the temperatures which could be withstood without failure, is in agreement with the experimental observations. For higher values of  $ah$  the index of merit can be reversed. For example, at an  $ah$  of 80, zircon becomes better than beryllium oxide, and for even higher values of  $ah$  beryllium oxide, which was quite good at the low values of  $ah$ , becomes the poorest of all the materials. This reversal is due to the fact that beryllium oxide has outstandingly good thermal conductivity, and that at the low values of  $ah$ , the index of merit takes advantage of this good conductivity. At the higher values of  $ah$ ,



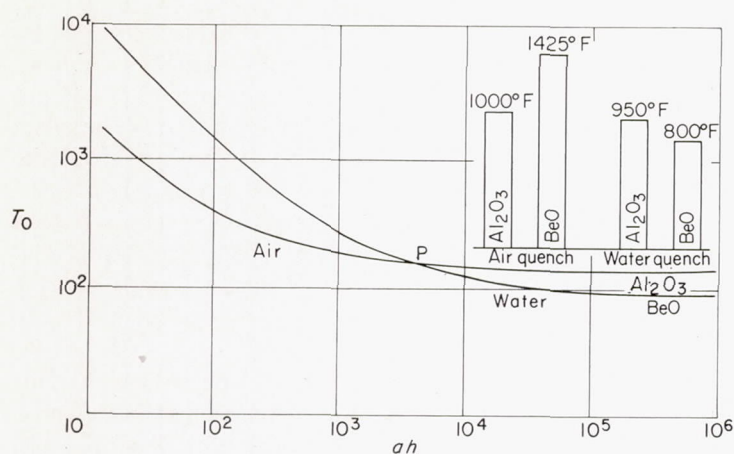


FIGURE 7.—Thermal shock tests of BeO and  $\text{Al}_2\text{O}_3$ .

the effect of the good conductivity gradually diminishes until at very high values the high thermal conductivity has no beneficial effect at all.

The importance of the possibility of reversal of merit index should be emphasized because it strongly suggests that the test conditions should simulate as closely as possible the intended use of the material. If, in order to obtain more rapid failure and thereby to expedite the testing procedure, more drastic conditions are imposed than the true application warrants, the order of merit of materials can be reversed, and the results rendered meaningless. The results of simple tests recently conducted at the Lewis laboratory will serve as experimental verification. The tests were conducted on specimens of beryllium oxide BeO and aluminum oxide  $\text{Al}_2\text{O}_3$  under two conditions of quench severity. All specimens were disks 2 inches in diameter and  $\frac{1}{4}$  inch thick and were quenched on their outer periphery while the sides were insulated. Air and water sprays were used as the quenching media. Figure 7 shows the analytical and experimental results. The curves show the variation of thermal shock resistance with quench severity for the two materials. These curves were obtained from equation (8) in conjunction with material properties listed by Bradshaw (ref. 5). For BeO these properties were appreciably different from those given in reference 4; hence, the curves for BeO in figures 6 and 7 are different. However, Bradshaw presents data for both BeO and  $\text{Al}_2\text{O}_3$ , and these data seem better to illustrate the experimental results. It is seen from figure 7 that for low values of  $ah$ , BeO is superior to  $\text{Al}_2\text{O}_3$ , but that for severe quenches BeO becomes distinctly inferior. This behavior is due, as previously mentioned, to the high conductivity of BeO, which is of value in improving thermal shock resistance primarily for mild quenches. At the severe quenches  $\text{Al}_2\text{O}_3$  assumes superiority owing primarily to its better relative breaking strength. The experimental results are shown in the insert in the upper right section of figure 7. In the air quench the superiority of BeO is evidenced by the fact that it withstood any temperature less than 1425° F, while the  $\text{Al}_2\text{O}_3$  failed at 1000° F. In the water quench BeO became inferior to  $\text{Al}_2\text{O}_3$ , failing when quenched from

800° F, while  $\text{Al}_2\text{O}_3$  withstood quenching until the temperature was 950° F. Because the actual air and water temperatures just before impingement on the specimens were not known, the true quench temperatures are not determinable, but qualitatively these tests certainly indicate the importance of quenching conditions on the determination of the relative merit of materials in their resistance to thermal shock.

Another interesting aspect of these tests is that the crossover point P between the two curves occurs very near the flat part of the  $\text{Al}_2\text{O}_3$  curve, at which point the BeO curve is still fairly steep. In these tests, the quenching conditions must have been in the region of the crossover point, because actual reversal of index of merit was observed. This may explain why the failure temperature did not change much in the two types of quench for the  $\text{Al}_2\text{O}_3$ , but appreciable change was observed for the BeO. Again, however, this conclusion must be considered very qualitative because the temperatures of the air and the water were not known.

**Stress at center of plate.**—Thus far only the maximum stress developed at the surface of the brittle plate has been discussed, and also it has been tacitly assumed that the duration of the thermal shock was sufficient to allow the maximum stress to be developed. For quenching from a high temperature, the surface stress is tensile, and in general, failure occurs at the surface. In the case of rapid heating, rather than rapid cooling, the surface stress is compressive, and surface failure may occur as a result of spalling, or as a result of the shear stress induced by the compression. Failure may, however, occur first not at the surface but at the center of the plate, where the largest tensile stress is developed. An important case is that in which the duration of the shock is not sufficient to allow the stress at the center to reach a maximum. Under this condition, the relative index of merit of materials of different conductivity depends on a criterion different from those already discussed; this criterion will now be explained.

A series of materials will be considered having similar geometry and identical physical properties except for thermal conductivity. It is desired to determine the center stress developed in a given time for each of these materials. The conventional plot of  $\sigma^*$  against  $\theta$  for given values of  $\beta$ , as used in figure 1, does not serve the present purpose because both  $\theta$  and  $\beta$  are functions of conductivity; hence, an examination of this type of plot does not readily reveal the significance of conductivity. The type of plot that best demonstrates the point is shown in figure 8. Here the dimensionless stress of  $\sigma^*$  at the center of the plate is plotted against the product  $\beta\theta$ . This product is also nondimensional, but since  $\theta$  varies directly with conductivity and  $\beta$  inversely with conductivity, the product is independent of conductivity and, for given  $h$ ,  $\rho$ ,  $a$ , and  $c$ , assumed to be the same for all materials; the horizontal scale depends on time only. The different conductivities do, however, correspond to different values of  $\beta$  ( $=ah/k$ ), and for the sake of demonstration three conductivities are shown having relative values 1, 2, and 10, or relative  $\beta$  values of 10, 5, and 1, respectively. It is to be



noted that the peak value of stress is lower the higher the conductivity, but that in the range of very low time, the curve for the material with the high conductivity lies above curves for materials with lower conductivities. Hence, if the surrounding high-temperature medium is allowed to act on the surface for only a short time, the tensile stress at the center will reach a higher stress the higher the conductivity.

The exact relative merit of the materials with different conductivities depends on the exact heating time. Thus, in figure 8 time ranges can be determined for which each material is superior to the others, and likewise time ranges can be found wherein each material is inferior to the others.

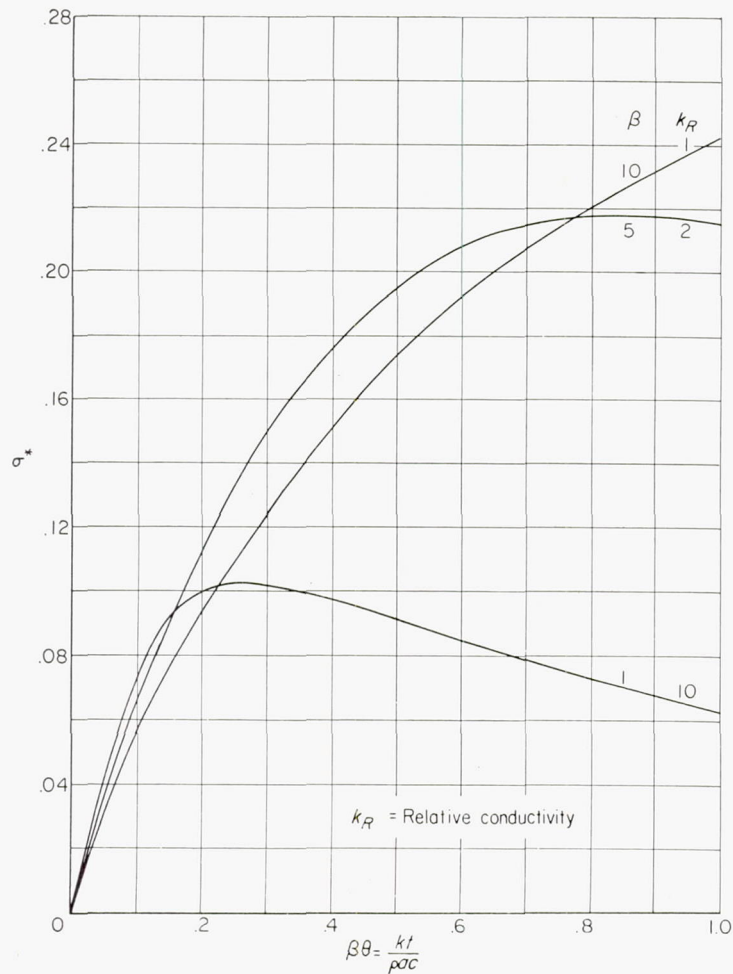


FIGURE 8.—Stress at center of plate.

It thus appears that, at least under certain conditions, good conductivity can be a detriment rather than an asset. A simple physical explanation for this phenomenon can readily be given: In the poor conductors only the fibers very near the surface are affected by the applied heating for the first very short interval of shock application. High stresses are thus induced in the surface, but these stresses are compressive and may not cause failure. The induced tensile stress at the center is low because the high compression of only a few fibers must be counteracted by the main bulk of the plate. For the better conductors the effect of the surface

heating is felt much more rapidly throughout the plate. The compressive stress at the surface may be lower at a given time, but more fibers are under compressive stress, and hence the induced tensile stress at the center is higher. The exact relative merit of materials with different conductivities depends upon the exact heating time, and no simple general formula has been found. Also it must be recognized that in the limit the trend must be reversed. Obviously a material with infinite conductivity must be the most desirable because in such a material no temperature gradients could be established, and no thermal stresses developed.

Bradshaw (ref. 1) discusses the condition in which poor conductors may have merit in connection with short-burning rockets. The application in this case is to a hollow cylinder, but the concepts involved are the same. Bradshaw, however, cites a very important point, namely, that in the poor conductors the surface temperatures may approach the melting point of the material even though the tensile stress at the center is lower than for the better conductors. The selection of an optimum material involves many considerations which must be studied in analytical detail before a final decision can be reached.

**Temperatures at time of maximum stress.**—One final consideration of interest to be discussed is the temperature distribution at the time of maximum stress. Consideration is again directed to the surface, and in figure 9 are shown the ratios of surface temperature to initial temperature and of average temperature to initial temperature as functions of  $\beta$ . Especially in the region of  $\beta$  from 0 to 1.0, which embraces a great many practical applications, the ratios are quite high. The maximum stress thus occurs when the temperature at the surface and the average temperature have not been reduced appreciably. From an analytical standpoint this result is of great importance because the physical properties of the materials considered often vary drastically with temperature. In particular, conductivity may undergo a many-fold change from room temperature to temperatures of the order of 2000° F. Deciding what conductivity to use in computations is therefore difficult. In the calculation of temperatures and stresses, it might be tempting, for purposes of simplification, to use the conductivity at a mean temperature between the initial value and that of the quenching medium. In view of the fact that the surface and mean temperatures are still quite high when the maximum stress is reached, however, this application would give incorrect results. The mean value to be used is that between the initial temperature and the temperature at the time of maximum stress. For example, if  $\beta$  is 0.4, the conductivity assumed should be the value at approximately 90 percent of the value at the higher temperature.

#### APPLICATION TO DUCTILE MATERIALS

The previous discussion was limited to brittle materials. In brittle materials the fact that stress is proportional to strain makes an analytical treatment possible; and the fact that failure can be achieved in one stress cycle makes it possible to obtain valid experimental results for correlation with



theory. When ductile materials are considered, the problem becomes much more complex. First, stress is no longer proportional to strain and therefore the stress equations cannot readily be solved. Only a few problems involving plastic flow of ductile materials under thermal stress have been solved in the literature. Second, it is rarely possible to obtain failure in one cycle. The failure process is a progressive one and material deterioration occurs during and in between applications of thermal shock. The metallurgy of the material becomes a predominating factor. Thus, with ductile materials the data are usually presented in the form of number of shock cycles withstood under a given set of conditions. As previously mentioned, thermal fatigue is very complex in brittle materials; it is even more complex in ductile materials as a result of metallurgical changes associated with plastic flow. In discussions of the thermal shock of ductile materials, reference can therefore be made only to the factors that are believed to be important. Even a determination of the pertinent variables should represent progress, however,

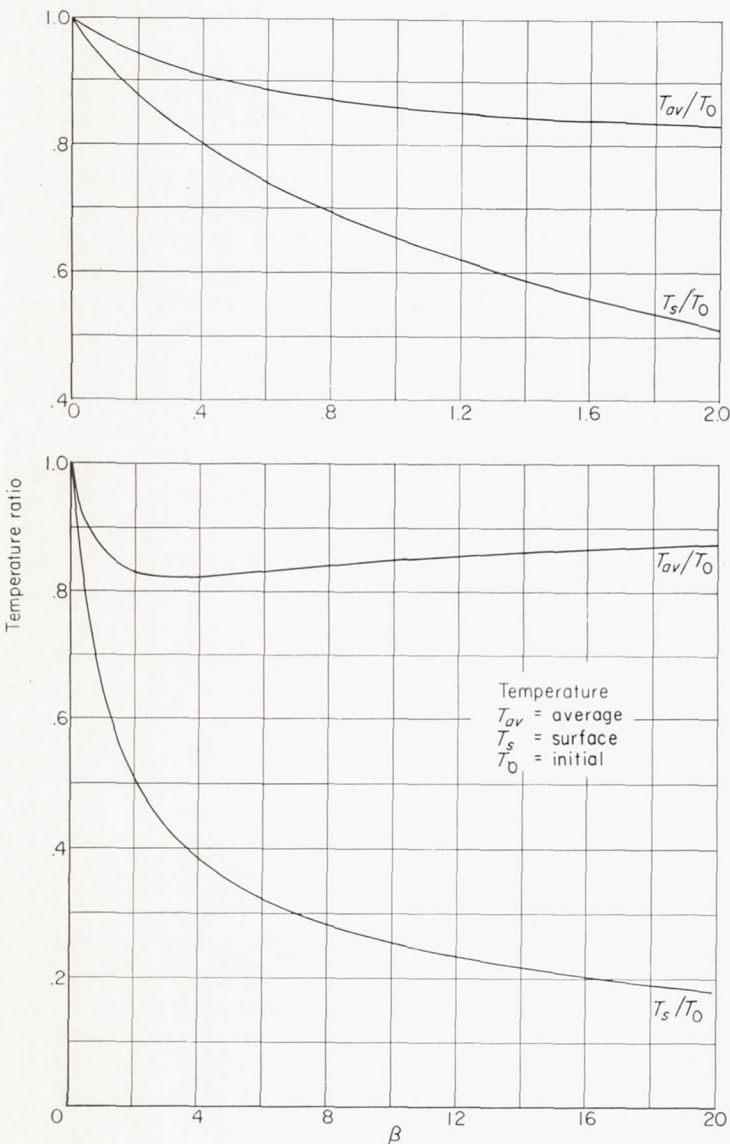


FIGURE 9.—Temperature ratio at time of maximum surface stress.

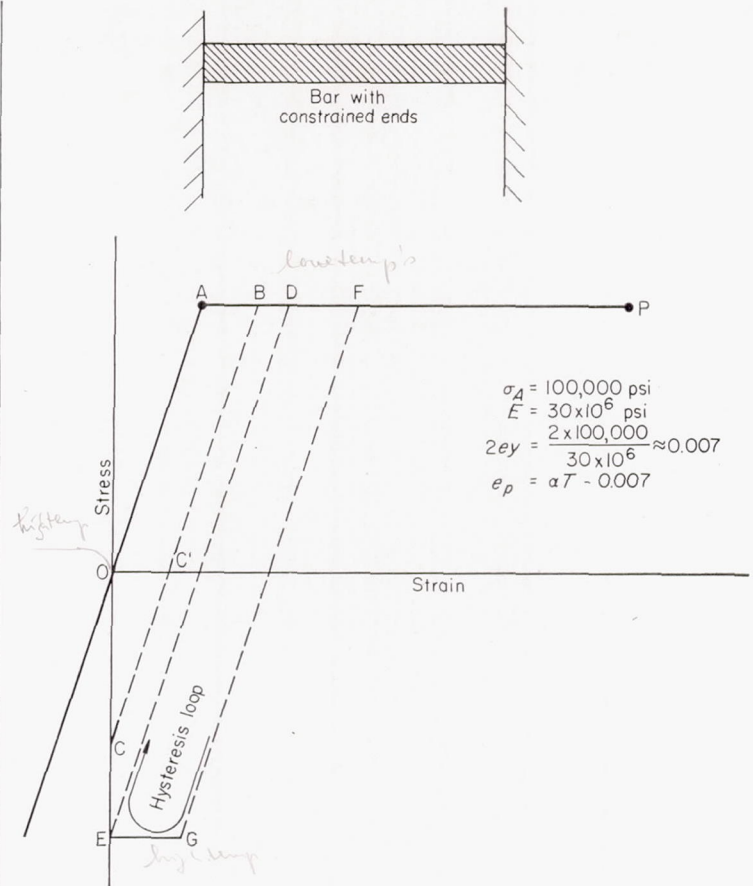


FIGURE 10.—Cyclic plastic strain in constrained bar due to heating and cooling.

since there are at present no critical tests in the literature that clearly define the role of these variables.

#### THERMAL CYCLING MODEL

One of the mechanisms associated with the ultimate failure of ductile materials in thermal cycling is plastic flow. The role of the plastic flow process can be outlined by considering a very idealized problem. The practical cases differ appreciably from the idealized problem, and later, the deviations of this model from the practical cases will be discussed.

In figure 10 is shown a bar fixed at its ends between two immovable plates so that the length of the bar must remain constant. This bar is assumed to be gradually cooled and heated between various temperature limits. Also shown in figure 10 is a hypothetical stress-strain curve for the material. It is assumed that the material is ideally plastic; that is, its stress-strain curve consists of a straight line up to the yield stress and further yielding occurs at a constant stress. Thus, in figure 10, stress is proportional to strain along the line OA and further strain takes place at stress  $\sigma_A$  until rupture occurs when the strain is P. Let it be assumed that at the start of the process the bar is unstressed in the hot condition, and it is subsequently gradually cooled. The bar is taken as stress-free in the heated condition in order to induce tensile stress during the first stage of the process.



If it were not constrained at its ends the bar would contract freely, and there would be no stress. Because of the constraint there must always be induced in the bar a strain  $\alpha T_0$  equal to the thermal expansion, and the stress will depend on this strain and on the stress-strain curve. As long as  $\alpha T_0$  is less than the strain A the stress is elastic, and analysis would proceed just as if the material were brittle. If the cycling temperature range is widened so that the thermal strain is equal to the strain at A, still no plastic flow would occur; and when the temperature is subsequently increased to its initial value, the stress would fall off to zero.

If, however, the cycling temperature range is increased to induce a thermal strain equal to that at B, the stress developed will be the yield stress, and plastic flow of an amount AB will be introduced during the first cycle of temperature reduction. When the temperature is again raised to its initial value the stress will fall along a line BC'C. Some time during the temperature increase the condition of the bar will be represented by C', where there is no stress but the strain is still not zero. When the initial temperature is finally reached the condition of the bar will be represented by point C—that is, zero strain and compressive stress OC, resulting from the fact that the free length of the bar had been increased by plastic flow by an amount AB. Subsequent cycling over this temperature range would cause the material to cycle between the points C and B and an indefinite number of cycles could be obtained without further plastic flow.

If the temperature difference of cycling produces a thermal strain twice the elastic strain, that is, the strain at D is

twice the strain at A, then cycling will occur between D and E, that is, between yield stress in tension and the yield stress in compression. (For simplicity, the yield stress in compression is here assumed to be equal to the yield stress in tension.) After the first cycle an indefinite number of cycles could be applied without further plastic flow.

Finally, consider an applied temperature difference such that the thermal strain is greater than twice the elastic strain, for example, point F. As the cooling cycle is applied the stress is first increased along the line OA and elastic strain occurs; then plastic flow occurs by an amount AF. As the specimen is subsequently heated it unloads elastically along the line FG. At G it still has not achieved its initial length because the strain is EG; and therefore as the temperature is brought back to the initial value, plastic flow at compression occurs by an amount EG. During the second cycle the stress first changes from the compressive yield stress at E to the tensile yield stress at D and then further tensile plastic flow DF occurs. On the second unloading cycle the material proceeds elastically from F to G and flows again in compression from G to E. Every cycle therefore induces in this bar plastic flow in tension of an amount DF and subsequently an equal amount of compressive plastic flow. This alternate compressive and plastic flow ultimately leads to failure of the material.

The question is the number of cycles of this kind that this material will withstand. A first estimate might be that the total amount of plastic flow in the material be equal to the initial amount of plastic flow that it could withstand in a conventional tensile test, that is, when the sum of DF and GE multiplied by the number of cycles is approximately equal to DP. This, however, would not be in agreement with the experimental behavior of materials. It has been found experimentally that the compressive plastic flow GE essentially improves the material so that even the sum of just the tensile components of plastic flow is greater than the ductility initially available in the conventional tensile test. That is, the summation of the DF values is greater than the strain DP. There is little quantitative information in the literature even on the simple problem of the amount of alternate plastic flow a material can withstand. A simple assumption can, however, be arrived at by a consideration of the data in a report by Sachs and coworkers (ref. 6). In this investigation 24S-T aluminum alloy was alternately stretched and compressed by the constant strain values and observation was made of the number of cycles that could be withstood before failure occurred.

Figure 11 shows typical results obtained in this investigation. The ductility remaining in the material after successive applications of cycles of 12-percent tension and compression is shown on the vertical axis; the number of cycle applications, on the horizontal axis. The remaining ductility, after application of various numbers of cycles of alternating strain, was measured by subjecting a precycled specimen to a conventional tensile test in which ductility was measured. It is seen that the alloy had an initial ductility of 37 percent.

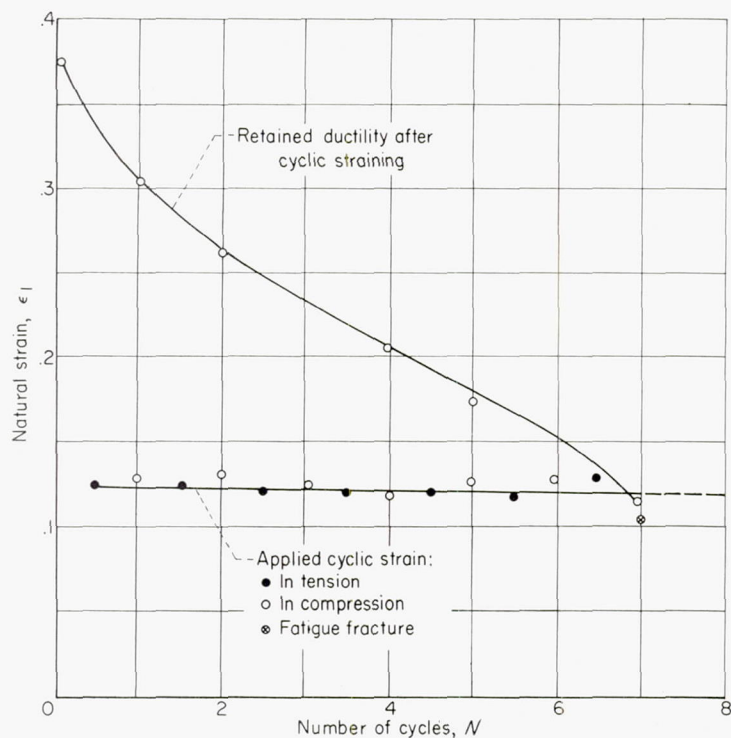


FIGURE 11.—Retained ductility of 24S-T alloy. Cyclic strain,  $\pm 0.12$  (from ref. 6).



After a 12-percent strain in tension and a 12-percent strain in compression were applied, the remaining ductility was reduced to 30 percent, a reduction less than that which would have been induced by just the 12-percent tension had not the compression followed. Similarly, it will be seen, each successive cycle reduced the remaining ductility by an amount less than 12 percent, and when the remaining ductility was less than 12 percent the specimen failed upon the succeeding application of the strain cycle.

A plot of the data contained in reference 6 leads to the relation

$$N = K/\epsilon^n \quad (14)$$

where

- $K$  proportionality constant
- $N$  number of cycles of plastic strain  $\pm \epsilon$
- $n$  exponent in the neighborhood of 3
- $\epsilon$  plastic strain

The number of cycles is thus inversely proportional to approximately the cube of the strain per cycle.

A table can be prepared for the relative number of cycles that a material might be expected to withstand in the thermal fatigue type of test previously described. A material having the following properties will be considered (see fig. 10):  $\alpha = 10^{-5}$  per °F,  $E = 30 \times 10^6$  pounds per square inch, and  $\sigma_y = 100,000$  pounds per square inch. The elastic strain that this material can withstand is 0.0033 inch per inch. As previously described, no cyclic plastic flow will occur until the imposed thermal strain is twice this elastic strain or, from the previously given values, until  $\alpha T \approx 0.007$ , or until the temperature is of the order of 700° F. It is now assumed that the imposed cycling is between 0 and 1000° F, 0 and 1200° F, 0 and 1400° F, 0 and 1600° F, and 0 and 1800° F; and the number of cycles will be determined in each case. These computations are as follows:

$$N_{1000} = K (1000 \times 10^{-5} - 0.007)^{-3}$$

$$N_{1200} = K (1200 \times 10^{-5} - 0.007)^{-3}$$

$$N_{1400} = K (1400 \times 10^{-5} - 0.007)^{-3}$$

$$N_{1600} = K (1600 \times 10^{-5} - 0.007)^{-3}$$

$$N_{1800} = K (1800 \times 10^{-5} - 0.007)^{-3}$$

Since these equations involve a constant  $K$  which is not known, only the relative number of cycles for each temperature can be determined. The results are shown in table II. If the number of cycles from 0 to 1000 is taken as a base line, the number of cycles for the 0 to 1200° F temperature range is reduced by a factor of 4.7; the temperature range from 0 to 1400° F results in a reduction factor of 12.6; from 0 to 1600° F, the reduction is by a factor of 27; and from 0 to 1800° F, the reduction is by a factor of 49.

Similarly, if the number of cycles at any other temperature range is used as a reference, the reduction in number of cycles for a higher temperature range is also shown in the table. The importance of this table is qualitatively to point to the drastic reduction in number of cycles to failure resulting from increasing the temperature range of cycling. Reference will later be made to some experimental results in the litera-

ture showing the importance of the effects of cyclic temperature range on the number of cycles.

#### IDEALIZATIONS IN THERMAL CYCLING MODEL

The foregoing analysis was idealized in many ways. First, the case treated was that of complete constraint; that is, no external expansion or contraction along the length of the rod was permitted. The entire thermal expansion was replaced by either elastic or plastic strain. Thus the problem represents a more severe case than most practical problems in which only partial constraint is imposed. (There are, on the other hand, cases in which the imposed strain is amplified as a result of geometric configuration, thereby imposing more severe conditions than complete constraint for a given temperature difference. Such a case will be discussed in a later section under "Size Effect.") Furthermore, strain hardening has been neglected, as was the fact that the stress-strain curve is very much a function of temperature, so that plastic flow occurs at different stress levels depending on the temperature. Also the yield stress in compression is usually different from the yield point in tension, and superimposed upon this is the fact that most materials exhibit a Bauschinger effect—that is, plastic flow in one direction reduces the stress at which plastic flow occurs in the opposite direction.

Added to these deviations is the fact that the mechanism of thermal shock failure may be different from that implicitly assumed in the foregoing model. Fatigue is generally thought of as a process of first initiating and then propagating a crack until ultimate rupture occurs. In the case of thermal stress cycling, the crack may not have to be initiated by the plastic flow; rather it may either be inherent in the part or it may result from metallurgical processes later to be discussed. Thus the role of plastic flow may be limited in this case to the propagation of the crack; or it may not even be necessary if the crack propagates by another mechanism. Probably the most important deviation of the practical case from the idealized case is that due to metallurgical effects which will now be discussed.

#### METALLURGICAL EFFECTS

During the thermal stress cycle, and between thermal stress cycles, the material is subjected to a complicated stress and temperature history that may cause metallurgical changes in the microstructure. Mention will be made of only several of the metallurgical processes that can occur. The whole subject of high-temperature metallurgy is really pertinent to this problem.

**Aging.**—Probably the most important action that takes place during and in between thermal stress tests is that of aging. Most high-temperature alloys in their use conditions are not in metallurgical equilibrium. In fact, it is because of their meta-stable condition that many alloys gain good high-temperature properties. If the material is maintained at high temperature, the tendency is toward rearrangement of the microstructure in the general direction of equilibrium. Thus, constituents that are in solid solution frequently tend to precipitate, and in so doing, they may drastically change



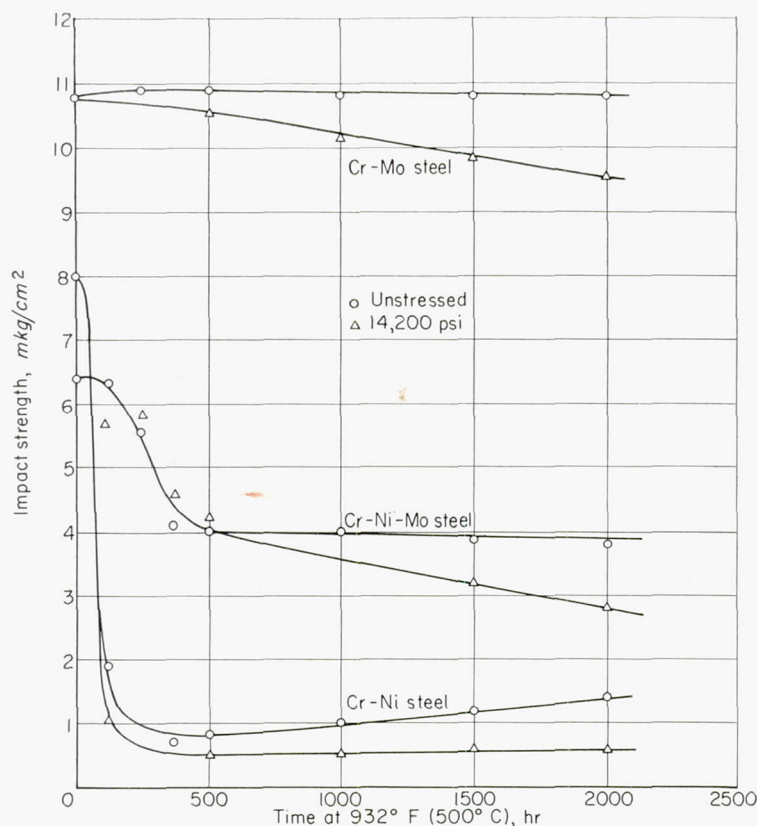


FIGURE 12.—Effects of heating with and without applied load on impact properties (from ref. 7).

the properties of the material. For example, they may precipitate in the grain boundaries and in this case they can reduce the ductility of the material, particularly in creep loading. This precipitation may occur with or without the application of stresses but generally stress tends to hasten the action. Finally, if the material becomes sufficiently embrittled, it may not be able to withstand even the small amount of plastic deformation required in a single thermal shock test. No careful investigations have, however, been made directly toward ascertaining the significance of precipitation in the thermal shock test. Its possible significance can be deduced by consideration of studies that have been made on the importance of precipitation in other types of mechanical tests.

Figure 12 shows some pertinent results originally published in the Russian literature and recently summarized by Sachs and Brown (ref. 7). Plotted are the impact strengths of three steels after they had been heated for certain periods of time at 932° F while in both the stressed and unstressed conditions. The impact strength has been found to be sensitive to precipitation embrittlement in cases when other types of tests miss detecting these effects completely. Note that heating alone of the Cr-Ni steel for about 100 hours reduced its impact strength tremendously. The presence of stress during heating caused this steel to embrittle even further. The Cr-Mo steel, on the other hand, showed little embrittling effect due to heating alone, with some embrittling resulting from the presence of stress. The stress was too low, however,

for any conclusive statements about the significance of stress. The Cr-Ni-Mo showed an intermediate effect between the Cr-Ni and the Cr-Mo steel. Nickel is known to be associated with temper brittleness, a phenomenon believed, but not proven, to be associated with grain boundary precipitation; hence, it is seen that precipitation may render an originally ductile material quite brittle. Of course, it would then become more susceptible to failure in thermal stress.

The main lessons to be learned from figure 12 are the importance of aging even without stress in reducing impact strength, and the importance of chemical composition on this effect. The aging need not take place during the thermal stress—it may occur during normal operation between thermal stress cycles. In laboratory thermal stress tests, it may occur during the heating periods or during high-temperature soaking—the important factor is time at temperature to allow the metallurgical reaction to take place. When the material is embrittled by all prior effects, thermal stress application will finally cause rupture. Since temperature is the most important variable affecting the aging process, any excessive temperatures introduced in order to accelerate testing may produce foreign results.

As for the importance of chemical composition, the indication is that initial properties do not necessarily govern thermal stress behavior. Thus the Cr-Ni steel had better impact properties before aging than the Cr-Ni-Mo steel, but aging had more drastic effect on the former steel. It is not surprising, therefore, that some materials seem to perform better in thermal stress tests when their conventional properties do not indicate any reason for the superiority.

**Corrosion.**—Another process that may reduce thermal stress resistance is chemical attack, known otherwise as corrosion, oxidation, and so forth. The surface of the material is usually in contact with oxygen or other gas capable of chemical reaction with the material. At the high temperatures involved in thermal stress testing, oxidation or other scales may form which are weak and brittle. Thermal shock testing then becomes a test, not of the original material, but of the resulting surface layer. Discontinuities formed at the surface layer either by cracking of the surface or by the disintegration of a corroded product act as a source of stress concentration that induces and propagates further cracks within the body of the material. In some cases the corrosion consists not of the formation of a surface layer, but of a diffusion into the body of the material. Hydrogen, for example, because of its small atomic dimension, readily diffuses into the grain boundaries of many materials, weakening them and rendering them less capable of withstanding thermal shock. The importance of intergranular attack is indicated by the fact that so many thermal shock failures are intergranular in nature.

**Hot and cold work.**—Thermal stress tests also embody hot and cold working of the material because of alternate thermal straining. This working is known to have important effects on the strength of the material and its subsequent properties. Figure 13 shows, for example, some results



obtained by W. Seigfried of Sulzer Bros., Ltd., Winterthur, Switzerland. In these tests the time to failure at 650° F was observed for a series of specimens at various applied stress levels. For smooth specimens the variation of life with stress is shown by line A. For specimens with a notch the variation of stress with temperature is shown by line B. Smooth specimens were then prestrained at room temperature by applying either 10 or 20 percent torsional strain. These specimens were then tested with or without notches, with results as indicated in the figure. For the smooth bar little reduction in life was observed, but for the notched specimens a tenfold reduction in life due to the torsion was observed, as shown by curve C.

The foregoing results are not directly applicable to analysis of the thermal stress process. They are presented merely to indicate that prior work can have an appreciable effect on subsequent time-dependent strength. In this case the effect is detrimental, although in many cases prior work improves the material. The significance of the notch in this case is that in thermal stress notches may bring out the importance of the prior strain history. Again, these notches may be design-incorporated, they may be due to corrosion or intergranular attack, or they may be the result of the early cracks formed in thermal stress testing.

**Grain growth.**—One of the effects of working is to render the material subject to recrystallization. When grains are broken up, energy is stored in the slip planes and in the grain boundaries, and upon subsequent heating there is a tendency for the material to recrystallize in order to achieve a state of lower stored energy. In many cases the effect is to cause grain growth. Figure 14 shows some data obtained by Rush, Freeman, and White (ref. 8) on the grain growth in the high-temperature alloy S-816 resulting from cold working. The plot shows the grain size resulting upon solution treatment at 2200° F as a function of the percent reduction per pass during the working process. It is seen that if the percent reduction per pass is approximately 0.75, which is a reasonable amount of plastic flow associated with a thermal shock cycle, the final grain size becomes A.S.T.M. minus 2 as compared with the original grain size, A.S.T.M. 5. Grain size A.S.T.M. minus 2 is such a large grain size that an average turbine blade might contain only several such grains per cross section as compared with approximately one thousand grains per cross section for grain size A.S.T.M. 5. Materials with high grain size generally have low ductility and would not be expected to have high thermal shock resistance.

In general, a number of thermal stress tests described in the literature indicated that there was no effect on the grain size. However, observations have been limited, and attention is directed to this factor as only one of the many complicated metallurgical processes that can occur.

Of greater importance, perhaps, is that accelerated tests at excessively high temperatures may cause grain growth to occur while operating conditions may not. Hence, an accelerated test might give misleading results.

**Residual stress.**—Another process that occurs in connec-

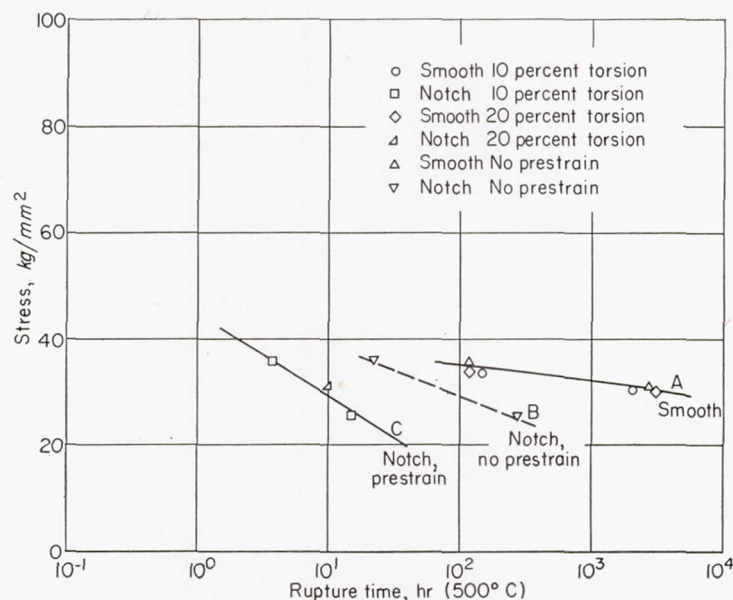


FIGURE 13.—Effect of working on strength of steel.

tion with thermal stress is the development and the relaxation of residual stress. As indicated in the previous simplified description of thermal cycling, the stress in a thermal shock test might be expected to oscillate between the yield point in tension and the yield point in compression. However, during and between the thermal shock tests, the temperature constantly changes and residual stress introduced under one set of conditions may be caused to relax under temperature relief at another temperature. An example will later be given of relaxation of initial residual stress in connection with conventional fatigue tests at elevated temperatures.

The foregoing discussion represents only the more obvious of the complicated mechanisms that can occur in a high-temperature material during thermal stress testing. If the metallurgical factor is accepted as being probably the most important in connection with thermal shock behavior of ductile materials, the significant conclusion to be reached relates to the importance of conducting tests to simulate actual operation. Metallurgical changes are very sensitive to time and temperature. If, then, an attempt is made to

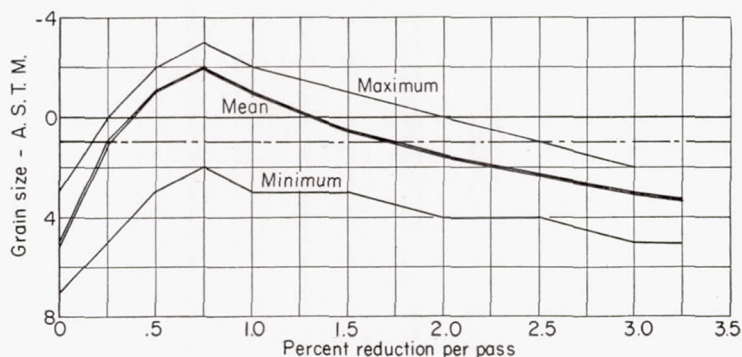


FIGURE 14.—Effect of prior critical deformation on grain size of S-816 alloy (from ref. 8).



render the test more severe in order to expedite failure, misleading results can be obtained because of the artificial metallurgical effects induced by the artificial test conditions.

#### EXPERIMENTAL INVESTIGATIONS OF DUCTILE MATERIALS

In most published literature on thermal shock of ductile materials, competitive materials are evaluated under a given set of conditions. From an engineering viewpoint, this is, of course, the most important type of test. From a fundamental viewpoint, however, the tests reveal very little information other than which material is better under the specified conditions. Some of the investigations do, however, lead to significant generalizations, and an attempt will be made to outline these results. Some of these tests will presently be discussed; others will be deferred until a later section on practical aspects of the problem.

##### NOZZLE VANES

Thermal shock tests that have been conducted in connection with gas-turbine nozzle vanes will first be discussed. The function of the nozzles is to direct hot gas at the proper angle against the rotating blades, which normally operate at temperatures in the neighborhood of 1600° or 1700° F. If for any reason combustion blow-out occurs, the gas is no longer heated and arrives at the nozzle diaphragm very much colder. The nozzle vanes are thus subject to thermal shock. Likewise, a certain amount of thermal shock occurs every time the engine is started because of the sudden application of hot gas to the nozzle vane surfaces.

One of the earliest investigations on nozzle vanes was published in 1938 in the German literature and was recently described in a survey by Bentele and Lowthian (ref. 9). Table III presents a summary of the results. The test consisted of a 1-minute heating cycle in a flame of gas and high-pressure air followed by a 3-minute cooling cycle in ambient air. These conditions do not simulate those associated with current aircraft jet engines, but they were satisfactory for the German application. Tests were conducted at two heating temperatures: one at approximately 650° to 700° C, and the other at approximately 850° to 900° C. The number of cycles under each of these two conditions is given by  $N_1$  and  $N_2$ . Under  $N_1$  distinction is made between failure due to distortion and failure due to cracking. These tests pointed out two important things: first, that excessive distortion is as important a type of failure as cracking, and second, that great decrease in the number of cycles resulted for an increase in test temperature of 200° C. As can be seen, there is, on the average, a reduction factor of more than 10 resulting from the temperature increase. This result is qualitatively in agreement with the previously presented simplified picture on the importance of temperature and attendant plastic strain on the number of cycles to failure. The high reduction factor may, in addition, be due to metallurgical effects introduced by the higher test temperature. Also of interest is the fact that the relative merit of the various materials changed with the test temperature. For example, specimen number 1 was nearly the

best at the higher test temperature, whereas it was poorest at the lower test temperature; on the other hand, specimen number 2, which was nearly the best at the low temperature, was one of the poorest at the high temperature. Further analysis of the data indicated that there was no relation between thermal shock resistance and ultimate tensile strength at room temperature, or the creep properties at 1300° F. Two materials, with tensile stresses differing by 23 percent, had the same thermal shock resistance; while two materials having practically identical creep characteristics had, respectively, the largest and the smallest

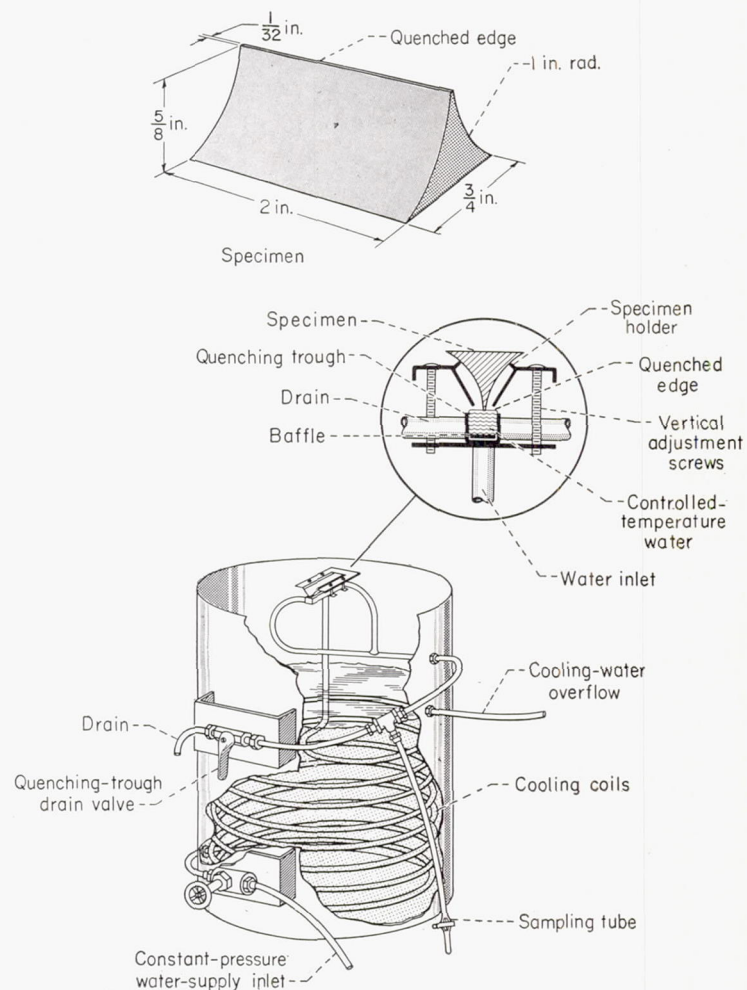


FIGURE 15.—Apparatus for quenching thermal-shock specimens (from ref. 10).

number of cycles to failure. These results point to the complexity of the factors influencing failure by thermal shock and indicate the probable importance of the specific metallurgy of the individual materials.

Another study of the thermal shock of nozzle blade materials was published recently in reference 10. The objective therein was to evaluate six cast high-temperature alloys for nozzle diaphragm application, and very extensive measurements were made in an attempt to analyze and interpret the data. Figure 15 shows the apparatus used in reference 10. The specimens were cast into somewhat triangular shape as



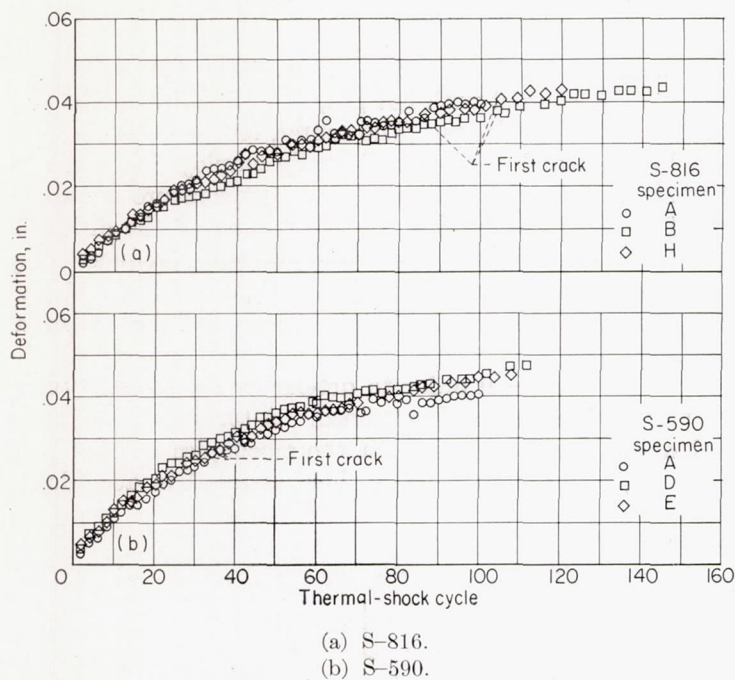


FIGURE 16.—Deformation produced in specimens by thermal shock (from ref. 10).

shown in the figure, the thin edge being  $\frac{1}{32}$  inch wide. They were first heated to a temperature of 1750° F and just the edge of the specimen was quenched in a flowing water bath maintained at a temperature of 40° F. The distortion of the specimen was measured both before and after cracking. Figure 16 shows a typical result obtained and indicates the fair consistency of the data; figure 17 shows a summary of all the results of the test. The distortion was measured as the height of bowing of the specimen. Considerable progressive deformation occurred after the initiation of the first crack. Also, the materials which were capable of greater distortion in the test lasted the largest number of cycles before breaking.

In order to analyze the results, the strains at fracture of the

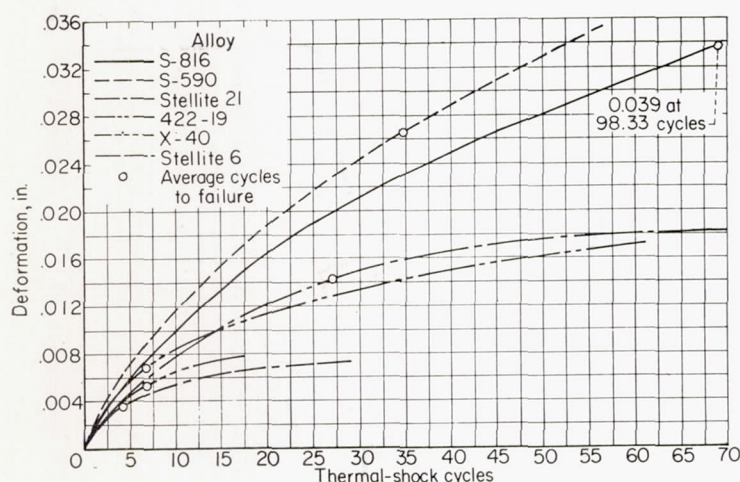


FIGURE 17.—Composite curves for progressive deformation of six alloys (ref. 10).

quenched thin edge were computed by assuming this edge to be the chord of a circle. Figure 18 shows the observed curvature in the specimens during cycling, and the assumption of circular shape was experimentally verified by use of an optical comparator. It was found that this strain was in all cases less than the ductility measured in the room-temperature tensile test. This result is to be expected for two reasons: First, the macroscopic strain is not a true measure of the total elongation of the material. As previously described in connection with the simplified model of the thermal stress failure mechanism, the plastic strain in the body is alternately tension and compression. In the case hypothesized in the model, no macroscopic strain would ever be measured since the ends were fixed for the very reason of preventing external dimension changes. Failure after thermal shock cycling occurs with low indicated ductility for the same reason that fatigue failures show little ductility—what plastic flow has occurred has been localized and alternating in sign, so that there is little external manifestation of ductility. A second reason that failure might have occurred with less indicated ductility than is obtained in the tensile

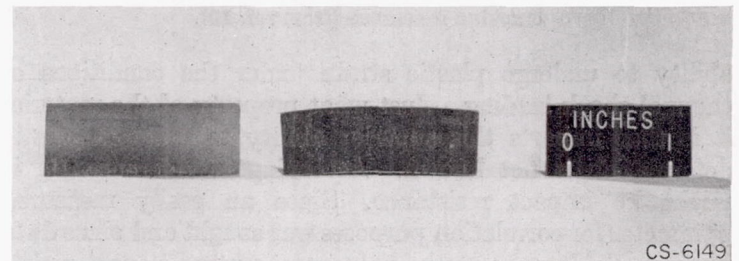


FIGURE 18.—Specimens before and after repeated thermal-shock cycles. Note curvature produced by thermal stress (from ref. 10).

test relates to the high-temperature embrittlement already discussed.

As a further analysis of the results, the reciprocal of computed strain at fracture was plotted on logarithmic coordinates against the number of cycles to fracture. The results are shown in figure 19, from which the following relation was obtained:

$$n = 4198 \Sigma_b^{1.318} \quad (15)$$

where  $\Sigma_b$  is the measured strain in the thin edge at fracture.

This is an important result, but unfortunately it does not present a criterion whereby materials can be evaluated before this very type of test is performed. The strain  $\Sigma_b$  bears no particular relation to the ductility of the material as measured in a conventional test, nor does it bear any known relation to any conventional physical property that can be determined without performing this very type of thermal shock test. Hence, there is no direct way of using this relation to predict in advance which is the better material. If the higher value of  $\Sigma_b$  is taken as an indication of greater plastic flow before thermal fracture, the superior performance in thermal shock may be considered as due to the superior



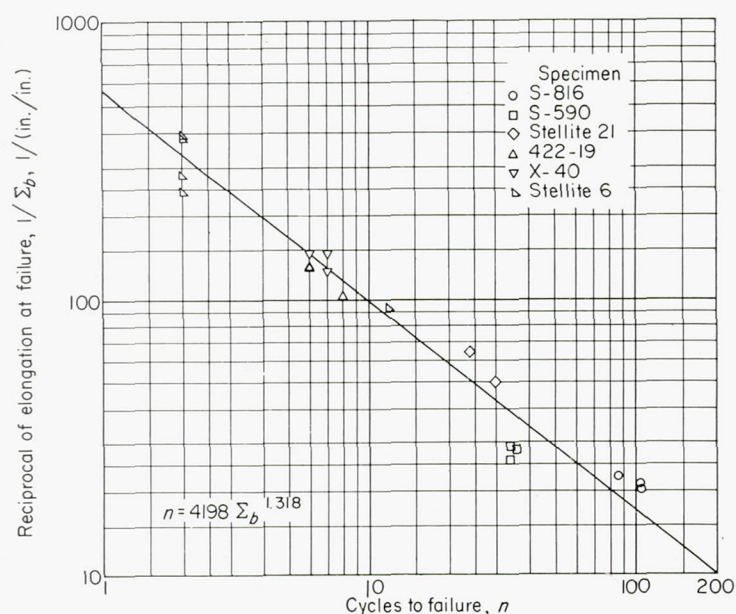


FIGURE 19.—Relation of reciprocal of elongation at failure to thermal-cracking resistance (from ref. 10).

ability to undergo plastic strain under the conditions of thermal shock loading. Just what property of the material it is that imparts this superior ability to undergo plastic deformation is not known. According to reference 10, it might be impact resistance. Since an easily measured parameter for correlation purposes was sought and since data were available only on the room-temperature impact resistance, these data were used for comparative purposes for a rough correlation, which is shown in table IV. Of course, the impact resistance that is of real importance is the impact resistance after the material has been subjected to the complicated thermal and mechanical history associated with this particular testing procedure, which has already been discussed. It is necessary to follow up this lead on the significance of impact resistance to verify the tentative conclusion reached in reference 10. It is not, however, an unreasonable conclusion since, as previously pointed out, the speed of loading in the thermal shock test may be an important factor, and this speed of loading is at least simulated in an impact test.

The most significant finding of reference 10 was the indication of the radically different behavior of six materials having, in the main, very similar mechanical and thermal properties. Thus, although it is not reasonable to conclude that neither the conventionally measured mechanical properties nor the thermal properties are significant in determining thermal shock resistance, it might be said that these properties combine with a third and very important type of property to produce an over-all thermal shock resistance. This third type of property is probably the metallurgy of the test material, as already discussed.

#### TURBINE DISKS

Another component of the gas-turbine engine which is subject to thermal shock, or at least thermal stress, is the

disk which carries the rotating blades. The rim of the disk is heated by contact with hot gas, as well as by conduction from the rotating blades. The center, on the other hand, is near bearings and cooling is generally employed in order to protect these bearings. A high temperature gradient therefore usually exists between the center of the disk and the rim. This high temperature gradient produces very large thermal stresses. Several investigations (refs. 11 and 12) were made to determine the significance of these thermal stresses.

**Temperatures.**—In order to determine the stress, typical temperatures were first determined. A turbine disk of early design was instrumented with thermocouples as shown in figure 20, and the engine was then operated in accordance

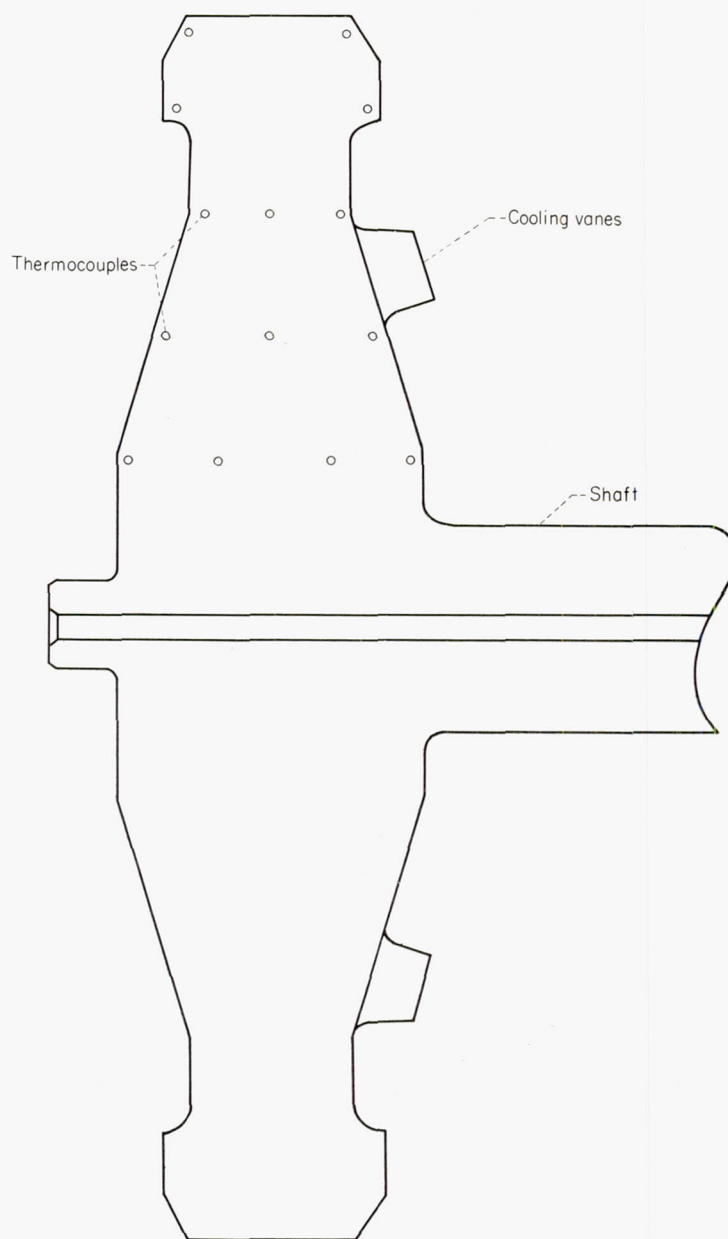


FIGURE 20.—Thermocouple location for study of disk temperature distribution (from ref. 11).



with a cycle shown in figure 21. It was brought up to idle speed of 4000 rpm in 1 minute, operated at idle speed for 4 minutes, then brought up in 15 seconds to a speed of 7500 rpm to simulate taxiing on the runway followed by a 2-minute idling at 4000 rpm to simulate operation while awaiting clearance for take-off. Finally, the engine was accelerated as rapidly as possible to rated speed of 11,500 rpm to simulate take-off conditions, and this engine speed was maintained for 15 minutes.

The measured temperature distributions are shown in figure 22. Along the abscissa is the disk radius in inches and along the ordinate, the temperature in °F. Each set of curves represents the temperature condition at some time after the start of engine operation. Three curves are shown in each set. The lower curve in each case is the temperature distribution along the face of the disk subjected to air drawn in by cooling vanes. The main purpose of this air flow is to maintain cool bearings. The upper curves show the radial temperature distribution on the uncooled face of the disk; the middle curves show the radial temperature distribution in a plane through the center of the disk normal to the axis of

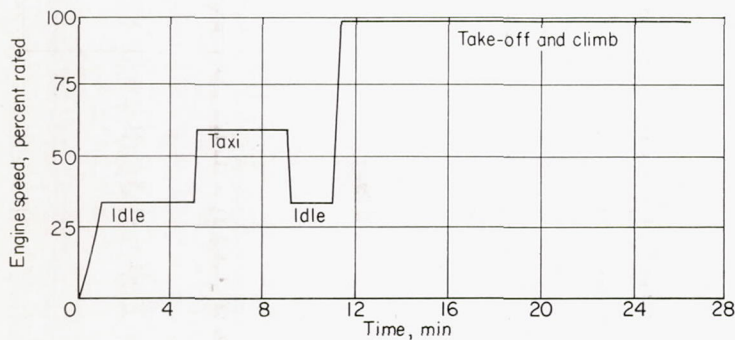


FIGURE 21.—Take-off sequence for turbojet engine (from ref. 11).

rotation. At the end of 10 minutes, during which time the engine was idling, the temperature at the hub of the disk was 90° F on the cooled side, 200° F in the center plane, and 400° F on the uncooled side. As the engine was brought up to full speed, the temperatures rose rapidly, as shown on these curves. The maximum temperature difference between the two faces of the disk reached 580° F at the end of 16 minutes.

**Stresses.**—Stress calculations were made with all three temperature distributions; for the present, those calculations will be discussed which were made with the temperature distribution on the cooled face of the disk because it represents the most severe case. In figure 23 is shown a centrifugal stress distribution in the disk at rated speed. These are the radial and tangential stresses due only to rotation. At the center of the disk, the stress is approximately 31,000 pounds per square inch. In figure 24 are shown the radial and tangential stresses with both the centrifugal and the thermal effect taken into account. Each curve shows the stress distribution at a different time after the start of the test; and for clarity separate plots have been made of radial and tangential stresses. It is seen that at the center of the disk the

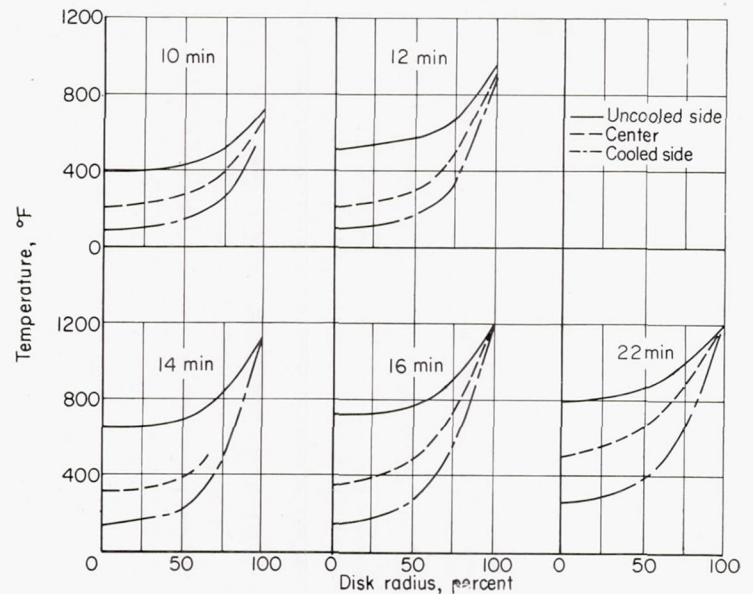


FIGURE 22.—Temperature distribution in turbine disk (from ref. 11).

stresses have been roughly doubled by inclusion of the thermal effect. They are now approximately 70,000 pounds per square inch. At the rim the stresses are very highly compressive. After 16 minutes, the elastic compressive stress at the rim is 120,000 pounds per square inch, which is much higher than the yield stress. Hence, plastic flow must occur in compression at the rim, calculations for which are shown in figure 25. After 16 minutes, owing to plastic flow, the stress is reduced to the neighborhood of 80,000 pounds per square inch compressive at the rim but at the center it is still of the order of 60,000 pounds per square inch tensile stress.

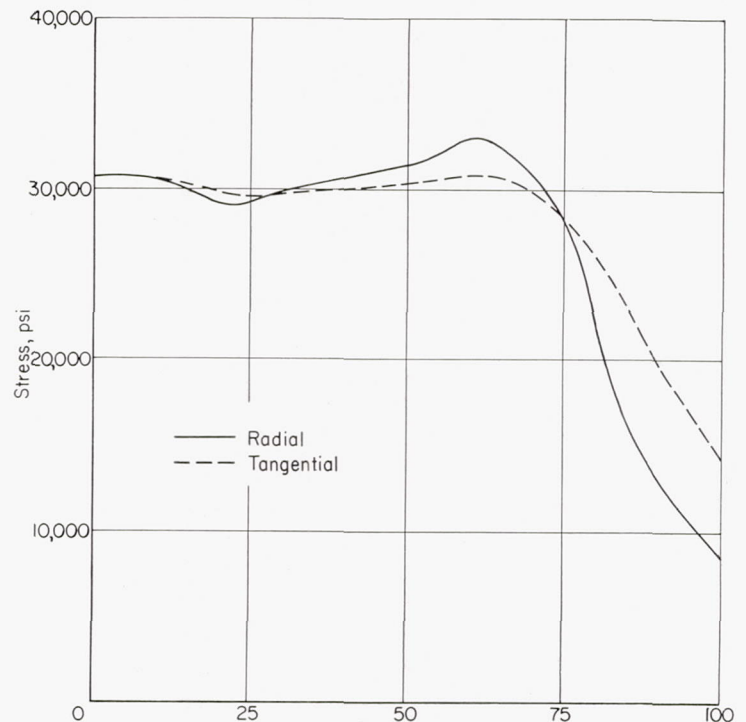


FIGURE 23.—Centrifugal stresses at rated speed (from ref. 11).



While the plastic flow has reduced the operating stress, it has introduced a new problem—residual stress when the engine is stopped. The free length of the rim has been effectively shortened by the plastic flow, and upon return to room-temperature conditions, the tendency of the remainder of the disk to force the rim to its initial length induces tensile stress. The computed residual stresses, again based on deformation theory of plasticity, are shown in figure 26. In these calculations the rim is assumed to be continuous; or, in effect, a wheel with welded blades is considered. The dotted curve shows the residual stress based on the computation of the temperature distribution in the center plane of the disk, and the dashed curve shows the residual stress distribution based on the temperature distribution in the cooled side of the disk. In either case, very high tensile stresses remain in the rim after engine stoppage. These high residual stresses coupled with the possibility of stress concentrations associated with blade fastenings may exceed the elastic limit of the material and cause further plastic flow in tension. Upon subsequent engine operation, plastic flow is in compression, and so on. Every time an engine is operated, alternate compressive and tensile plastic flow may take place. This plastic flow, together with metallurgical changes occurring as a result of

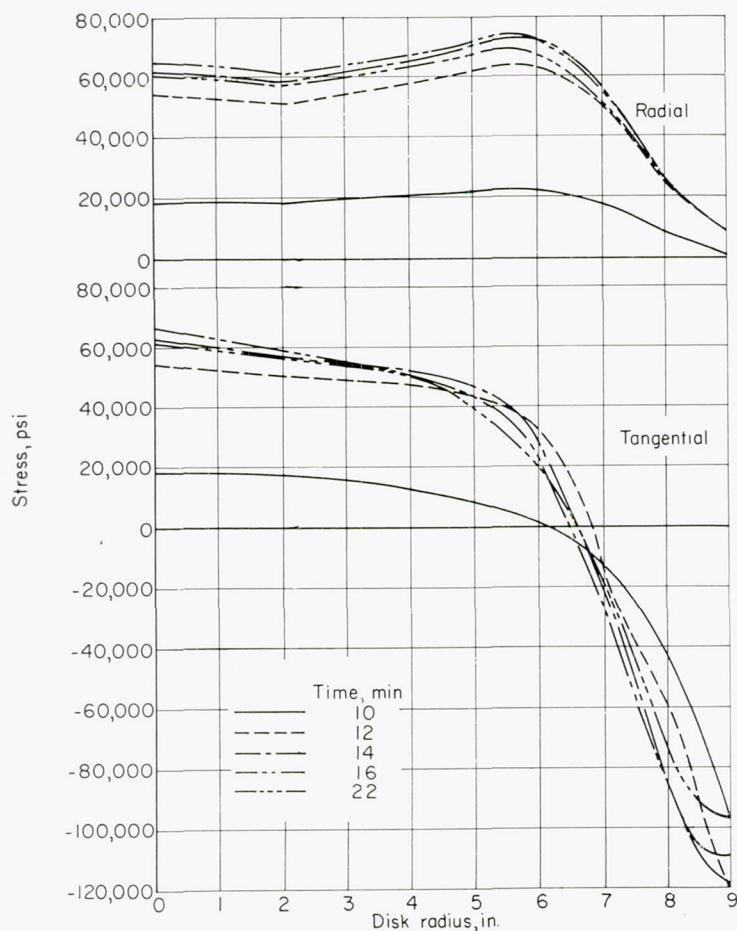


FIGURE 24.—Elastic stresses for temperature distribution on cooled side of turbine disk (from ref. 11).

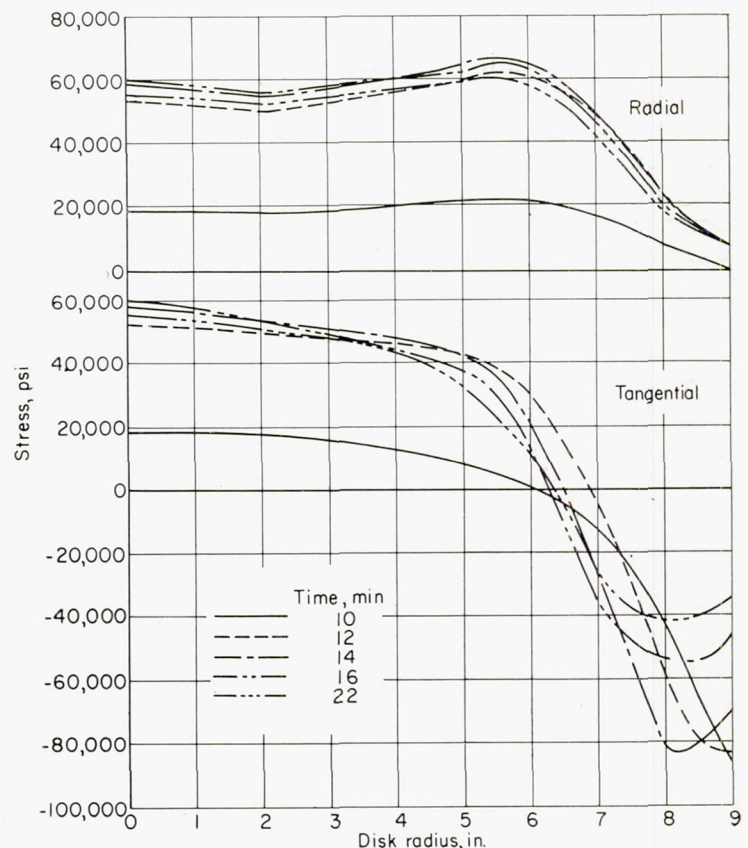


FIGURE 25.—Plastic stresses for temperature distribution on cooled side of turbine disk (from ref. 11).

engine operating temperatures, may ultimately result in rim failure.

**Effects on rims with inserted blades.**—The effect of the thermal stress depends primarily on the design of the wheel. Two types of designs have been used in this country, the most popular of which has the fir-tree-type blade fastening. Figure 27 shows a close-up of such a blade attachment, as well as cracks that occurred at the base of the attachment as a result of alternate tensile and compressive plastic flow. Such cracks are not common in wheels with fir-tree attachment; in fact, there has been no evidence of such failures in fir-tree wheels until very recently. These particular cracks occurred in connection with a program that required cycling between idling and full power three times per hour. The wheel had withstood nearly 1000 hours or 3000 cycles before these cracks occurred. Note that these cracks occurred on the cooled side where the temperature gradient and stresses were at a maximum. When detected, the cracks had not yet progressed through the thickness of the wheel to the uncooled side. Even in wheels with fir-tree attachments, thermal stress cracks can occur.

Other effects of thermal stress in fir-tree wheels relate to blade loosening and tightening. When the blade is made of a material having approximately the same, or a higher, coefficient of thermal expansion as the wheel, and when the initial fit between blade and wheel is moderately tight, the



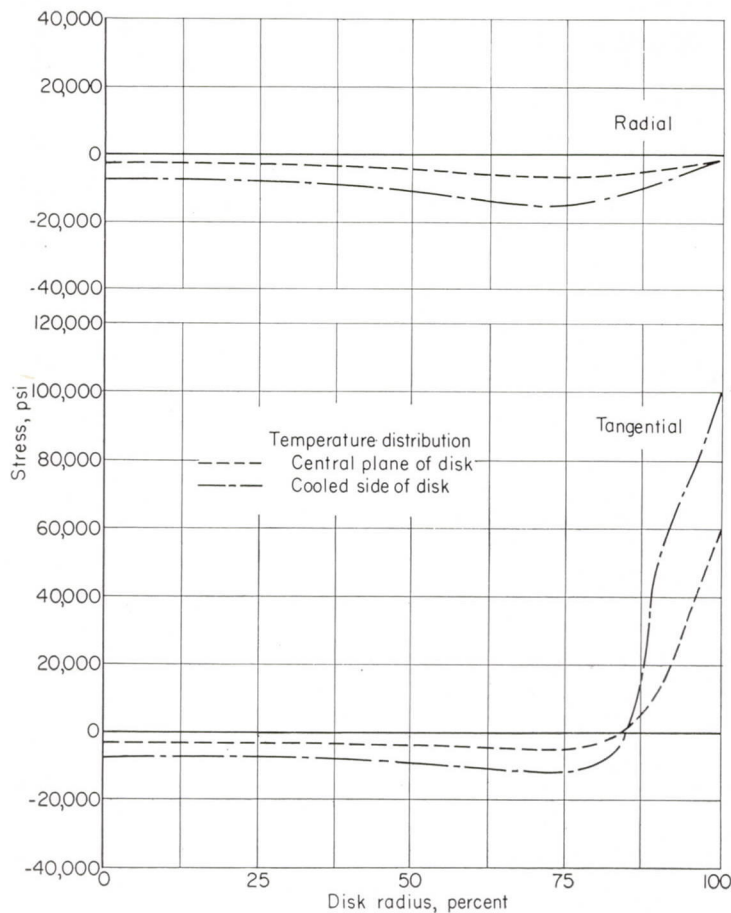


FIGURE 26—Residual stresses after operation (from ref. 11).

blades are generally found to be loose in their mounts after they have once been run. This loosening is due to the fact that compressive plastic flow in the rim has effectively shortened the length of serrated segments of both blade and wheel. Upon return to room-temperature conditions, the tendency is for the blades to pull away from the wheel lands. In the case of the welded blades, this is not possible because the blades are an integral part of the wheel and therefore tensile stresses result. In wheels with the fir-tree type of blade, however, it is possible for the blades to pull away from the wheel. Hence, in doing so they become very loose under stationary conditions. They might tighten up, however, upon returning to operating conditions.

In other instances fir-tree blades have become even tighter in their mounts than when initially inserted. This fact was at first considered strange in the light of the prior experience of loosening already discussed. Upon investigation it was found, however, that tightening occurred only when the coefficient of expansion of the blade material was much lower than the coefficient of expansion of the wheel material. Thus, when the wheel is at operating temperature the blade bases, which do not expand so much as the wheel lands, essentially shrink away from these wheel lands. The compressive

stresses due to thermal temperature gradient in the disk have to be absorbed, therefore, in the wheel region below the blade fastening rather than in the blade fastening area, as when the blades had approximately the same coefficient of expansion as the wheel. Upon return to static conditions the plastic flow causes the region immediately below the rim region to become smaller than its initial size; the disk lands are thus pulled somewhat in toward the center of the disk. The blades are therefore tightened.

**Effect on rims with welded blades.**—In the case of wheels with welded blades, not only is the full residual stress developed because the blades cannot pull away from the rim, but there usually are present stress concentrations produced by discontinuities between adjacent blades. Thermal cracking has thus been a severe problem with such wheels. The small rim cracks in figure 28 resulted from engine operation with a typical early welded wheel. To prove that these cracks were the result of thermal stress and not the effect of rotation, the wheel was alternately induction-heated and cooled to simulate engine temperature gradients without rotation. Some of the cracks progressed appreciably, as shown in the figure. Several potential remedies for rim cracking of disks with welded blades will be discussed in a later section. At the present time, the tendency has been to abandon the welded blade construction in favor of the fir-tree-type of attachment. This trend is partly due to problems of blade replacement in the field, but primarily it is because of the problem of thermal cracking.

**Effect on bursting.**—Thus far the effect of thermal stress has been considered only in the rim region of the disk. The question arises as to its importance at the center of the disk. In the disk previously described, the stresses at the center were roughly doubled by the presence of the temperature gradient. It is conceivable that these thermal stresses may

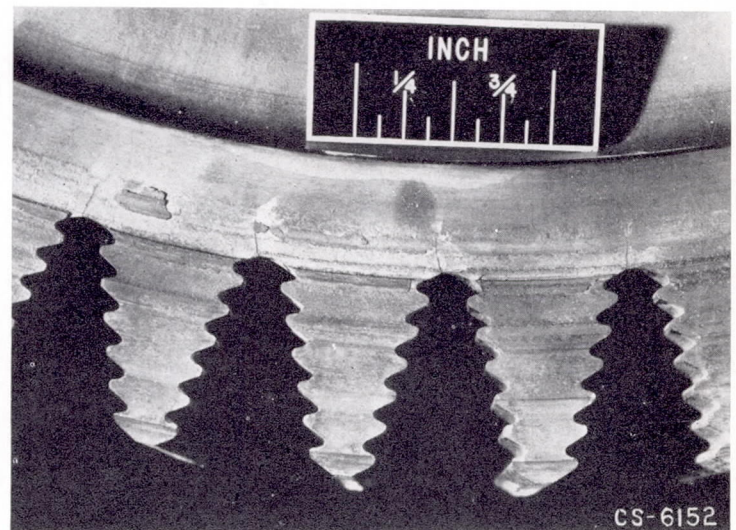


FIGURE 27.—Thermal cracks in turbine wheel with fir-tree blade attachments.



cause the disk to burst sooner as a result of overspeed. In order to determine whether or not these thermal stresses could affect the burst speed, an investigation was undertaken on simple parallel-sided disks which were tested to destruction in a spin pit (ref. 12). With the deformation theory of plasticity as a basis, the speed at which the disk with temperature gradient would burst was computed and compared with the speed at which the disk without temperature gradient burst. It was found that very little effect should be expected. Although the thermal stresses and the centrifugal stresses were additive at the center of the disk at low rotative speeds before plastic deformation, the thermal effect gradually vanished as the speed was increased, provided the material had appreciable ductility (say, over 3 percent). Near the burst speed, the stress distribution in the disk with temperature gradient was effectively the same as the stress distribu-

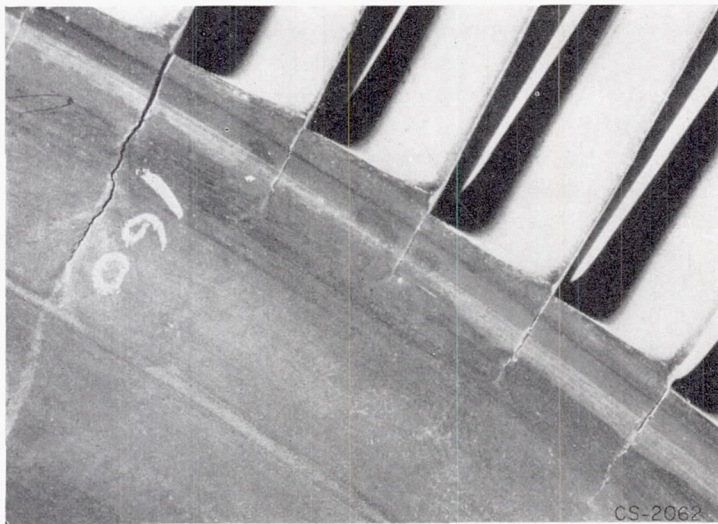


FIGURE 28.—Cracks in welded turbine wheel after 15 induction heating cycles (from ref. 11).

tion without temperature gradient. Some of the results of the computations are shown in figure 29. Only the tangential stress distribution is plotted because it best reflects the thermal effect. The dashed curve shows the stress distribution for the centrifugal stress only; the solid curve shows the total stresses including the thermal effect. It should be noted that at the low speeds there is appreciable difference between the two stress distributions; but as the burst speed is approached the two stress distributions become practically identical. When the plastic strain due to centrifugal stress is large, it overshadows the thermal strain, and there is little effect on stress distribution.

Figure 30 shows a comparison between experimental results and theoretical computations of the effect of temperature gradient on burst speed. Neither the theoretical nor the experimental results indicate a very significant effect of temperature gradient; what influence is present is due primarily to the effect of temperature on material properties, rather than to thermal stress.

This investigation emphasizes the importance of cycling in the thermal stress problem compared with the single application of thermal stress in a material of moderate ductility.

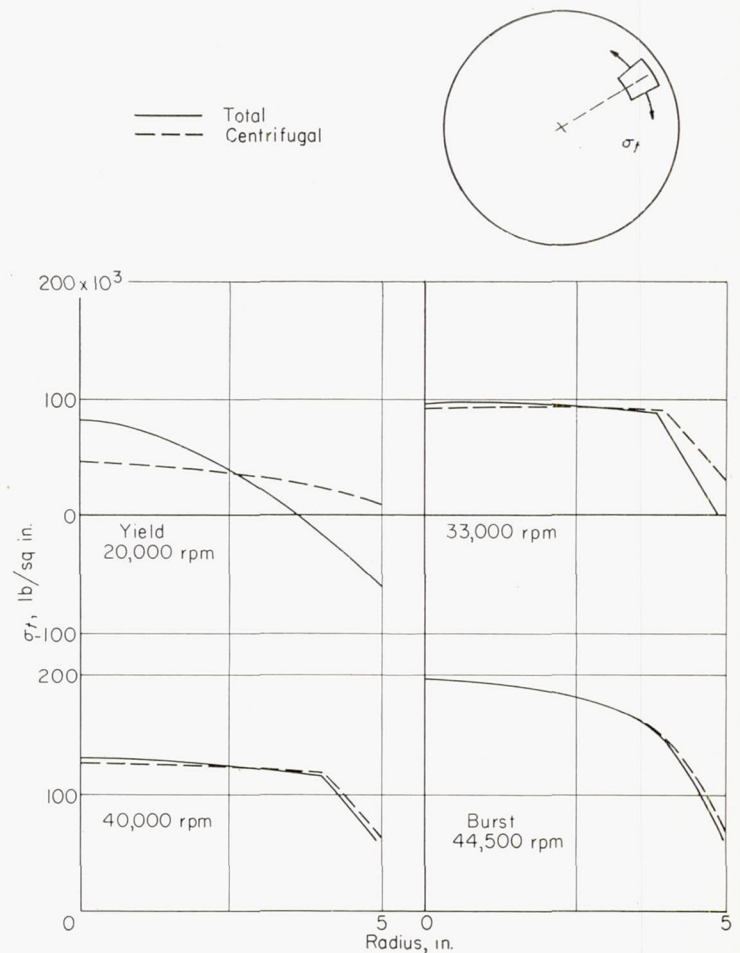


FIGURE 29.—Comparison of total tangential stress with centrifugal tangential stress (from ref. 12).

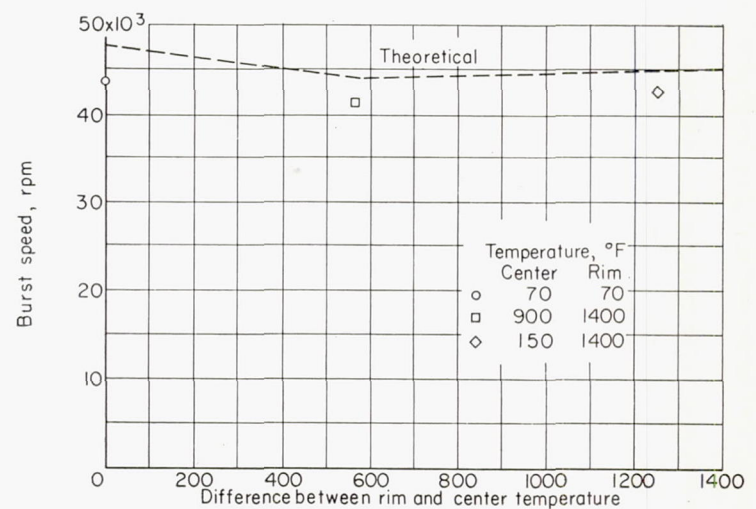


FIGURE 30.—Burst speeds of disks with temperature gradient (from ref. 12).



## LOCOMOTIVE WHEELS

The problem of thermal cracking of locomotive wheels is nearly identical with that of the turbine wheel. During braking action these wheels must absorb so much energy that the rims rapidly become heated to temperatures in the vicinity of 1000° F before the temperature at the center of the wheel is appreciably raised. Thus, compressive thermal stresses are induced at the rim, with attendant plastic flow, and residual tensile stress occurs upon return to uniform temperature. After a sufficient number of cycles, rim cracking occurs which rapidly spreads, finally causing total wheel fracture. Figure 31 (ref. 13) shows typical wheel fractures produced in service. To prove that these fractures were associated primarily with thermal cracking, laboratory tests were conducted simulating the thermal gradients, and wheel fractures such as those shown in the lower half of figure 31 were obtained.

Reference 13 presents considerable discussion of the thermal stress problem, and further reference will be made to this work in the remaining section of this report.

## SOME PRACTICAL ASPECTS OF THERMAL SHOCK RESISTANCE

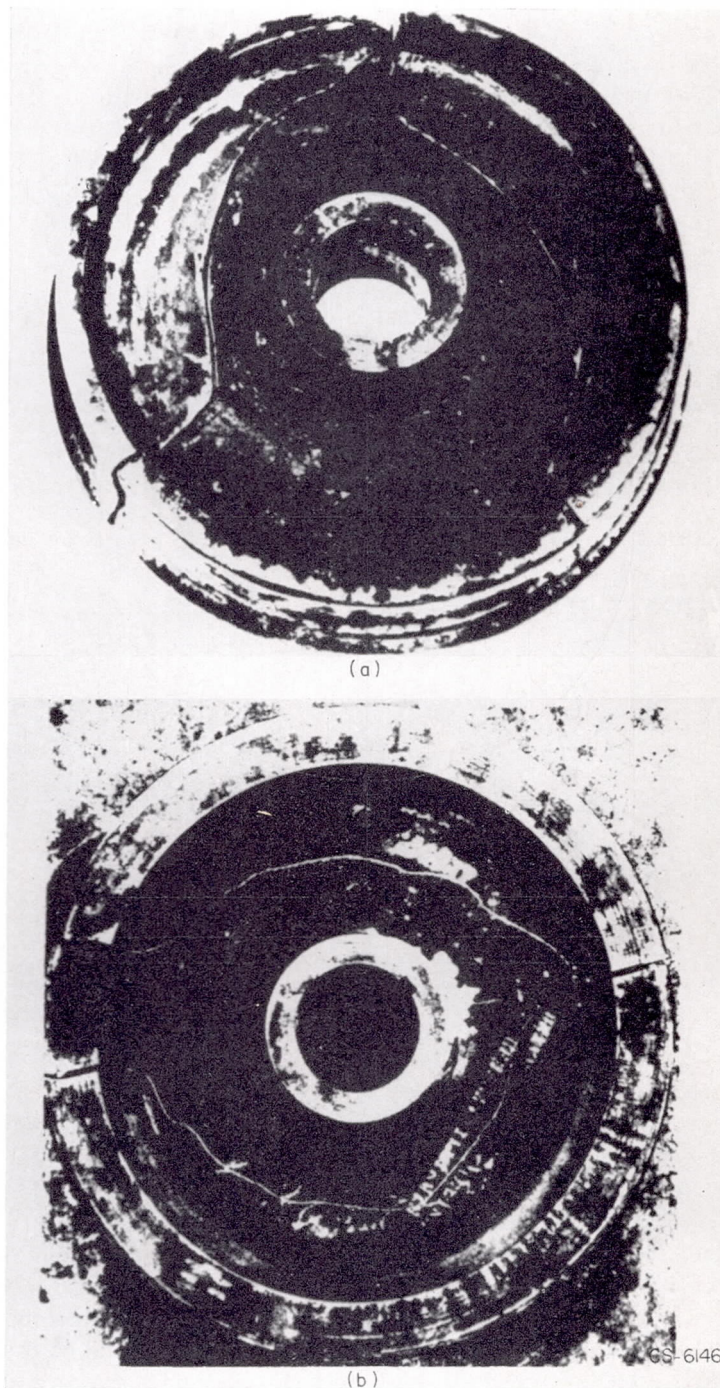
Throughout the report the emphasis has been on the complex nature of the thermal shock phenomenon, especially as related to ductile materials. It is desirable now to summarize some of the aspects of this problem that have, from a practical standpoint, been found to be important. Illustrative examples will be drawn from the literature. The variables discussed are, in the main, the components of the simplified thermal shock formulas, equations (7) and (8).

## EFFECT OF STRESS CONCENTRATION

In brittle materials the stress at a point of stress concentration is usually the governing stress leading toward failure. Hence, stress concentrations are certainly of the greatest importance in the thermal shock of brittle materials. In ductile materials, stress concentrations are not of the utmost importance for a single application of loading, but become as important as in brittle materials as the load is applied cyclically. As previously discussed, thermal failure in ductile materials generally occurs only after several applications of the shock loading. Hence, stress concentration is of great importance even in ductile materials. This is especially true if the metallurgy of the material is severely affected by localized plastic flow. Several illustrations of the importance of stress concentration will be presented from experimental evidence in the literature.

**Turbine disks.**—In some cases the geometry of a part is such as to make stress concentration inherent. Frequently it is possible, however, to provide a measure of relief, for example, by drilling of a stress-relieving hole at the base of the notch. The case of the turbine disk with welded blades has already been cited as one involving inherent stress concentrations. A laboratory investigation (ref. 14) was conducted to follow up the rim cracking problem in disks

subjected to high temperature gradients. In this investigation, series of stress concentrations of different magnitudes were imposed by providing discontinuities of different types



(a) Wheel fracture produced in service.

(b) Wheel fracture produced in the laboratory.

FIGURE 31.—Typical wheel fractures (from ref. 13).

at the surface of the disk, as shown in figure 32. These disks were parallel-sided and of 13½-inch diameter; and semi-circular notches of three different radius sizes as well as sharp 60° notches were machined into the surface. The



failures always occurred first at the base of the sharpest notch. These tests were followed by attempts to improve the resistance of the disks to thermal cracking by drilling small holes beneath the base of the notch. In general, it was found that these holes had a beneficial effect in at least retarding the initiation and propagation of the cracks.

**Combustion-chamber liners.**—Another investigation that pointed out the importance of stress concentration in thermal

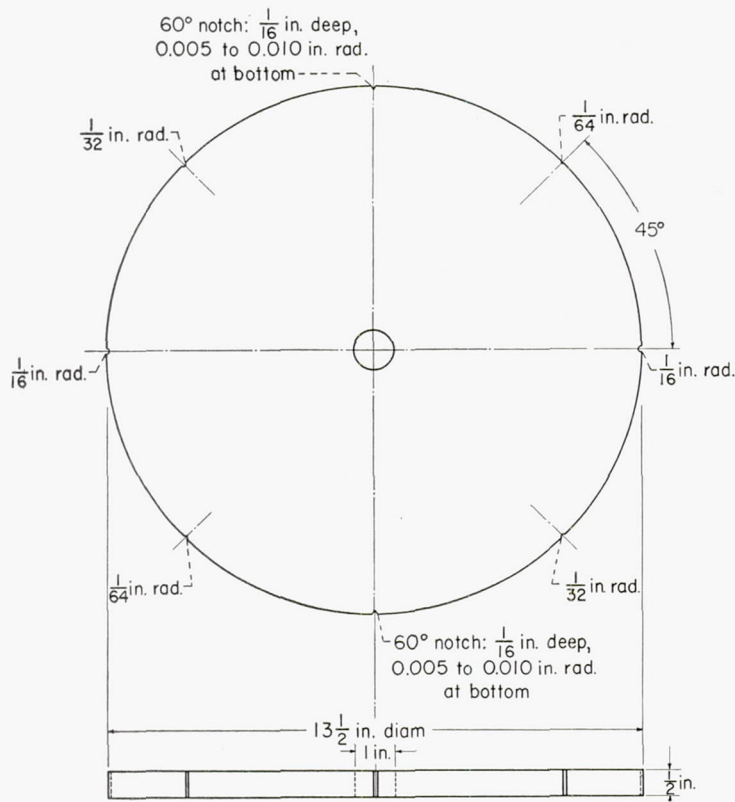


FIGURE 32.—Notched-rim disk used in thermal stress investigation (from ref. 14).

fatigue was described in reference 15, which concerns the determination of the mechanisms of failure of turbojet combustion liners. Such liners, shown in figure 33, serve the purpose of properly distributing the air into the combustion chamber. The circular holes feed the air into the combustion chamber, and the louvers shown in the center of each of the two combustion liners cool the liner in the areas between the holes. These louvers are fabricated by first punching the liner and then bending the flap out of the plane of the liner. The geometry of the louver can better be seen in figure 34, which is a photograph of the louver as well as of the stress-relieving holes at the base of the louver. Also shown are various types of cracks that occur in operation. Although the circular holes are intended for relieving the stress at the effective notch present at the base of each louver, it was found that the fabrication of these holes by punching introduced highly worked metal and irregularities in the periphery of the hole that acted as further stress concentrations.

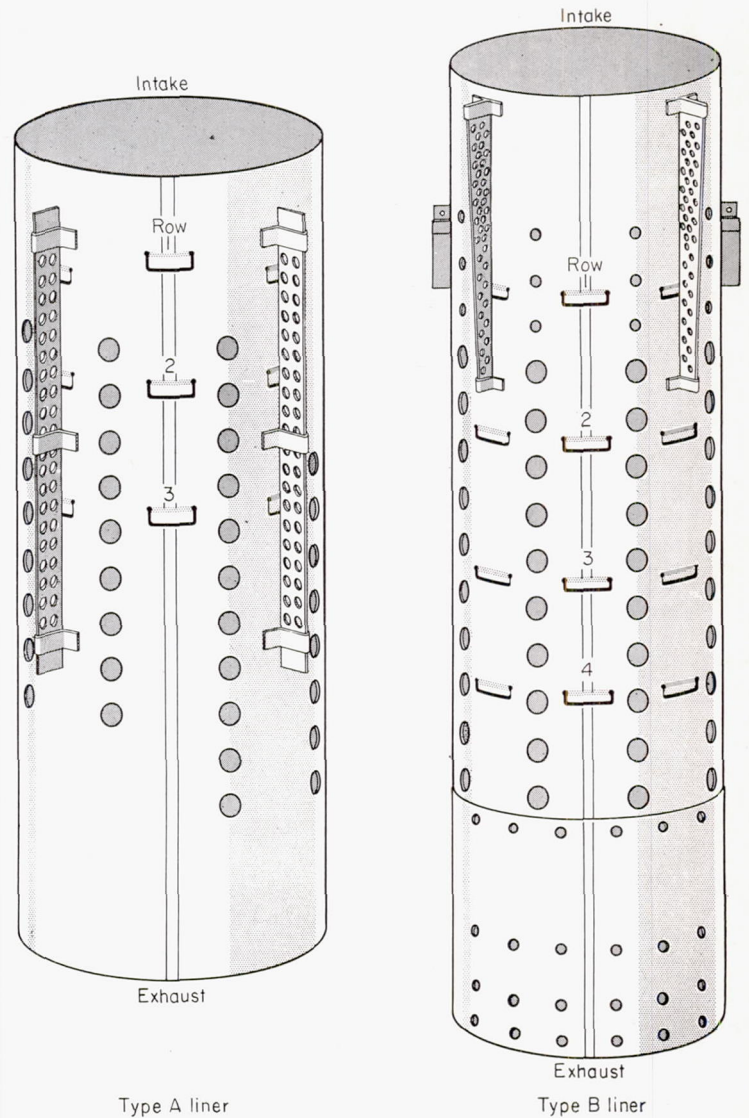


FIGURE 33.—Combustion-chamber liner construction (from ref. 15).

By reaming, sanding, and vapor blasting the punched edges, the resistance to thermal cracking was vastly improved. Table V shows the experimental results where a comparison is presented of the number of cracks measured in seven liners in the as-fabricated condition and seven liners in the improved condition. A large reduction occurs in the number of cracks at the two inspection periods conducted after 8 hours and 20 minutes and after 16 hours and 40 minutes of engine operation.

**Stress concentrations resulting from operation.**—In some cases the stress concentrations are not built in, but are produced as a result of operating conditions. For example, surface attack can produce discontinuities that act as stress concentrations. In an investigation on the thermal shock resistance of nozzle blades, Bentele and Lowthian (ref. 9) found that if the test blades were polished and etched after every 250 cycles in a mild chemical solution, the crack resistance was vastly improved. They attributed this improve-



ment largely to the removal of surface irregularities by the mild chemical change without, however, an appreciable attack by the chemical on the grain boundaries. Prior tests in which aqua regia had been used to remove surface scale for inspection purposes had definitely reduced thermal shock resistance of the material and led to early intercrystalline cracking. These results point to the importance of surface attack, and in a later section the possibility of avoiding such attack by the use of surface coatings will be discussed.

#### EFFECT OF CONSTRAINTS

Thermal stresses result from constraints that prevent free expansion of the various sections of the part under consideration. While in many cases the constraint is inherent in the physical continuity of the part, it frequently is possible to incorporate some measure of relief by proper design. Following are several illustrative cases.

**Turbine wheels.**—In the turbine wheel, for example, the use of the fir-tree-type attachment enables the designer to provide a loose fit between the blade and disk. The clearance can then be used for at least partial expansion in the rim region where the temperature is the highest. Even in turbine disks with welded attachments, it is possible to improve the thermal stress resistance by providing a slot (fig. 35)

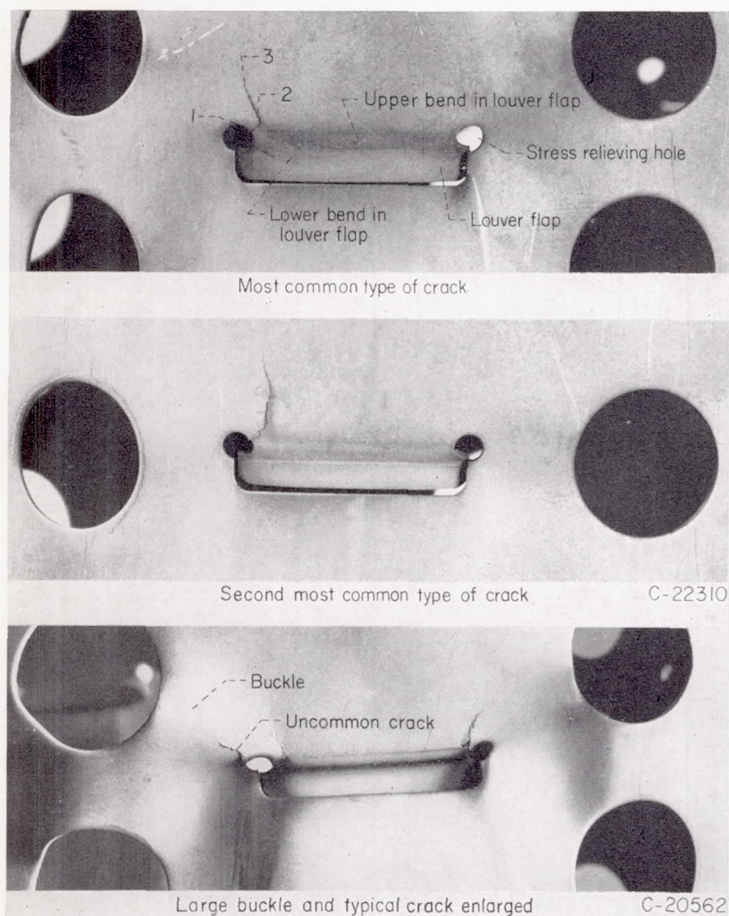


FIGURE 34.—Typical cracks and buckle at louver (from ref. 15).

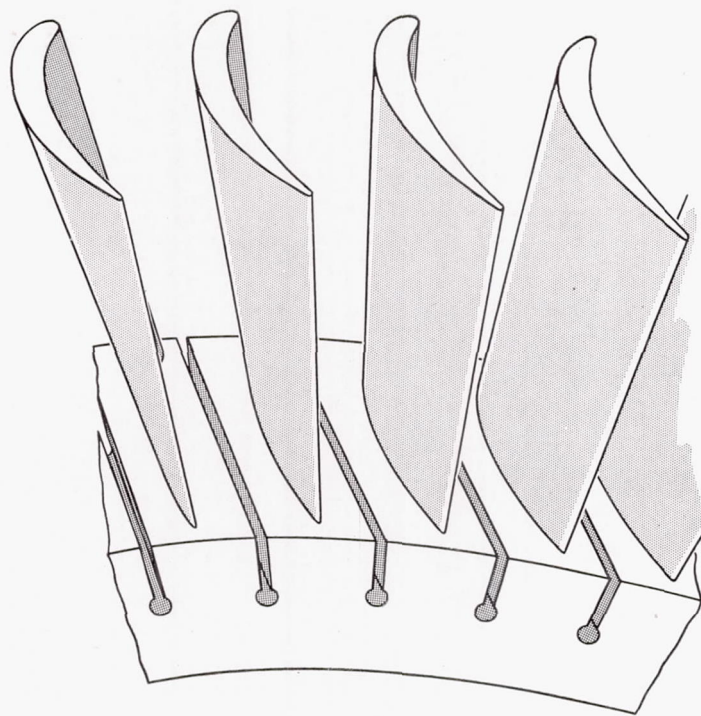


FIGURE 35.—Welded blade attachment with keyhole slots (from ref. 11).

between the blades. The hot rim may then expand and partially close the slot. The use of stress-relieving holes at the base of the slot probably is good practice.

**Turbine nozzles.**—In turbine nozzle vanes, constraint is sometimes minimized by means of the arrangement shown in the right side of figure 36. The left side shows an early form of design in which the nozzle vanes are welded at both ends onto thick rings. The outer ring is at lower temperature and therefore does not expand so much as the blades. Free expansion of the blade is thereby prevented, which condition induces high compressive plastic flow followed by residual tensile stress; successive repetition produces thermal fatigue failure. If the nozzle vane is floated in cut-out sections of ring, the blades can expand freely and the ring serves only to position the blade.

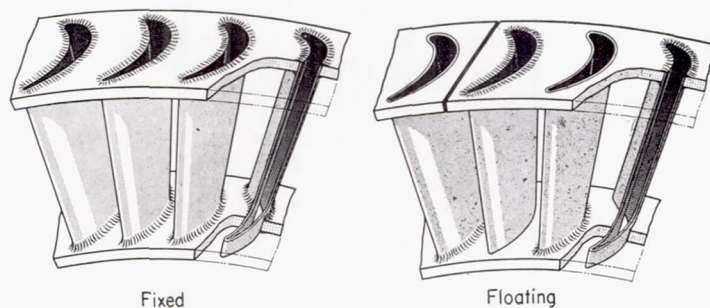


FIGURE 36.—Nozzle diaphragm.



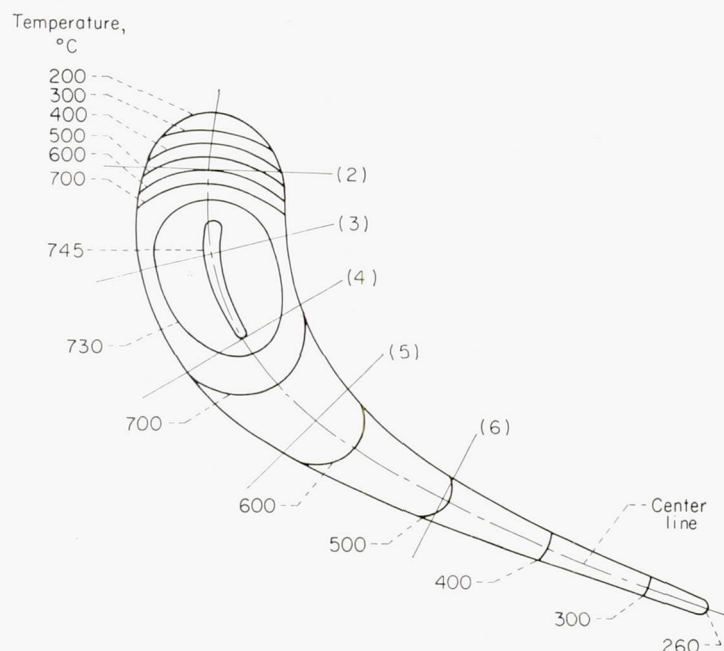


FIGURE 37.—Calculated temperature distribution in blade after 4 seconds cooling (from ref. 9).

It should be emphasized, of course, that this free-floating design does not completely remove stress in thermal shock because the blade still does not cool uniformly when subjected to a blast of cold air. Figure 37 shows the computed temperature distribution in a nozzle vane investigation by Bentele and Lowthian (ref. 9). This temperature distribution was computed for a time 4 seconds after the application of an air blast onto the blade initially at  $850^{\circ}\text{C}$ . The surface is, of course, at a much lower temperature than the interior of the blade. By idealizing the geometry of the nozzle vane and computing the stresses by an approximate method, Bentele and Lowthian found an elastic stress of over 100,000 pounds per square inch tension near the leading edge. This stress was well above the elastic limit of the material and obviously plastic flow must have occurred. The location of ultimate failure in thermal cycling agreed with the predictions based on elastic stress analysis.

The use of hollow nozzle vanes probably improves thermal shock resistance by reducing thermal inertia and by evening out temperature distribution. Air cooling through the hollow vanes, of course, further improves the thermal shock resistance, but even without cooling the hollow blades should give better performance in addition to reduced weight and strategic material content considered so important at the present time.

#### SIZE EFFECT

Large size is really nothing more than the addition of constraint, since in a body of large size the portion undergoing rapid temperature change is generally prevented from expansion or contraction by a massive section which does not perceive the imposed temperature change for an appreciable

period of time. A laboratory investigation conducted to study size effect on brittle materials will now be described, and then several practical cases involving size effect will be discussed.

**Laboratory investigation on brittle materials.**—Figure 38 shows some test results to demonstrate size effect in brittle materials. The tests were conducted on geometrically similar specimens of steatite, cooled in such a manner that they acted essentially as infinite hollow cylinders rapidly cooled at their outer surface. The specimens were first heated to a uniform temperature and then quenched at their surface by air, and in other tests, by water. The initial temperature difference between the specimen and the coolant required to cause fracture in one cycle was measured. An analysis, similar to that shown earlier for the flat plate, can readily be made to indicate that this initial temperature difference should vary linearly with the reciprocal of diameter, which is well verified in figure 38. For a given specimen diameter the water quench, which is more severe and for which the value of  $\beta$  is greater than for the air quench, required lower initial temperature differences to produce failure. Both straight lines intersect the vertical axis at a temperature value of approximately  $250^{\circ}\text{F}$ . The intercept on the vertical axis represents the case of infinite size, or complete constraint, and the value of this intercept

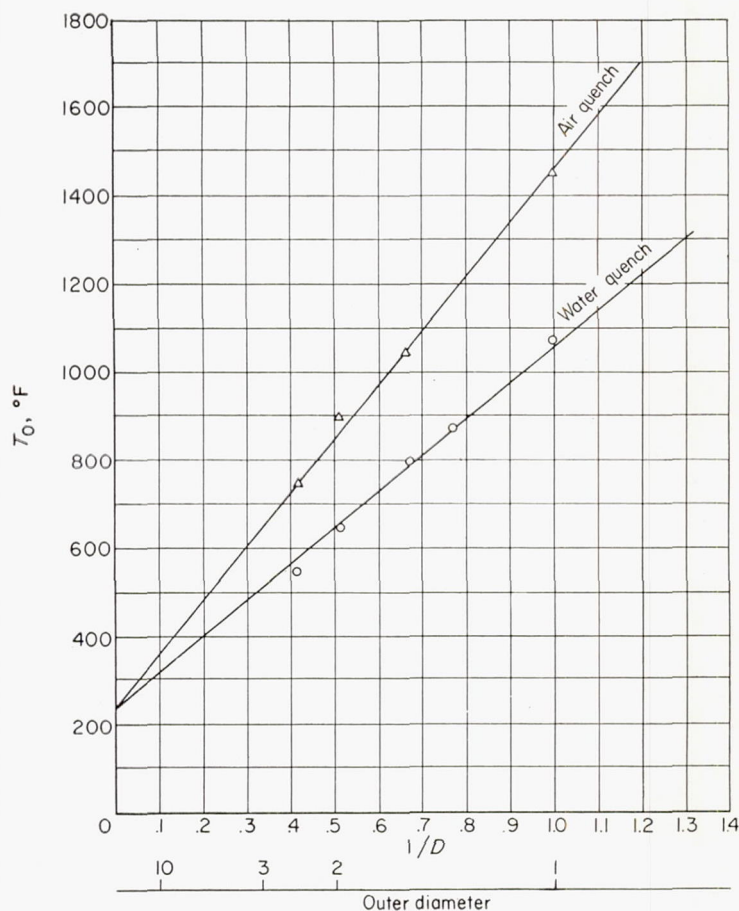


FIGURE 38.—Size effect in thermal shock of steatite.



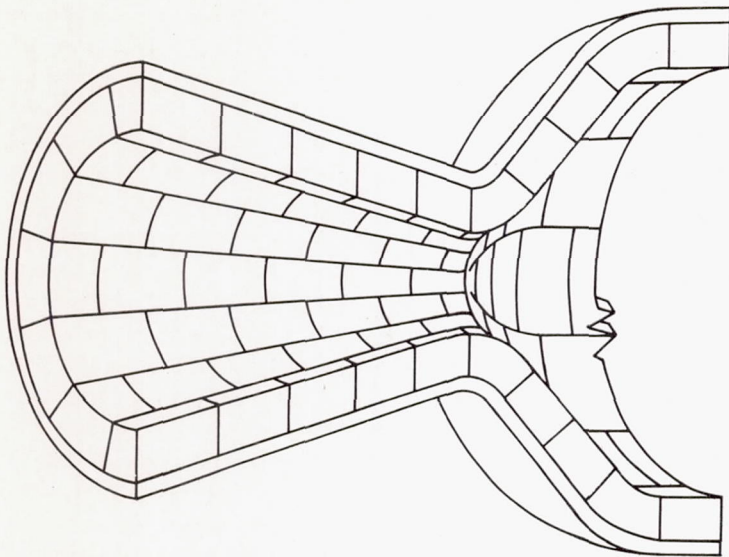


FIGURE 39.—Thermal-shock resistant rocket nozzle.

should be  $\sigma_b/E\alpha$  for steatite. Based on the data given by Buessem (ref. 3), the value of  $250^\circ\text{F}$  is in good agreement with the theoretical value for this material.

Figure 38 is presented chiefly to demonstrate the reciprocal nature of thermal shock resistance to size, and also to point out that there is a temperature difference below which failure will not occur, even for infinite size.

**Built-up structure.**—In some cases it may be possible to minimize size effect by building up a large structure from small units, each of which is highly resistant to thermal shock because of its size. Figure 39 shows a conceivable arrangement for a rocket nozzle liner. The small blocks might have to be lightly cemented together, or held together by a wire mesh, for mechanical reasons; thermally they

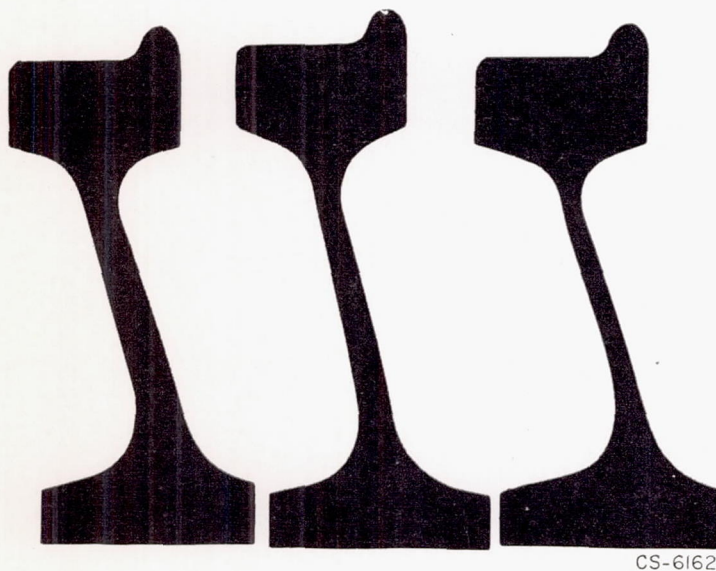


FIGURE 40.—Cross sections of thick, intermediate, and thin plate wheels (from ref. 13).

would act independently and they would be greatly superior in thermal shock.

**Effect of massive cores.**—Temperature changes are usually imposed at the surface; it is prevention of expansion or contraction by the inner core that induces thermal stress. The use of hollow nozzle vanes in this connection has already been referenced; other examples can be found in the locomotive wheels and the turbine disks. Figure 40 shows three locomotive wheels investigated by Schrader and coworkers in reference 13. All wheels have the same hub and rim, but the thickness of the plate, which connects the hub to the rim, has been varied. The reasoning here was that as the rim is heated by the braking action its free expansion is prevented by the plate. Hence, a thinner plate might offer less constraint and thereby improve life.

The results of the tests of reference 13 are shown in figure 41. Three conditions of heat treatment are shown, and in all cases the  $\frac{1}{2}$ -by  $\frac{5}{8}$ -inch wheel, the thinnest of the three, lasted by far the greatest number of test cycles.

Likewise, figure 42 (ref. 11) shows the results of some analytical studies on turbine disk profiles. The solid profile is the disk previously described, and the solid lines represent the radial and tangential stresses in this disk based on the measured temperature distribution in the central plane. The dotted profiles represent redesigns that reduce the weight as well as the stress.

**Effect of localized strain absorption.**—In some cases geometrical configuration dictates that the total thermal elongation of a large portion of a body be equaled by the elongation of a small section. The unit elongation or strain in the smaller section is thus greater than the strain in the larger section. Figure 43 schematically indicates a simple case of this type. Sections B and C are assumed to be of equal temperature, but lower than that of sections A by a value of  $T_A$ . If the entire body is unstressed when at uniform temperature, the thermal elongation  $\alpha_A T_A l_A$ , where

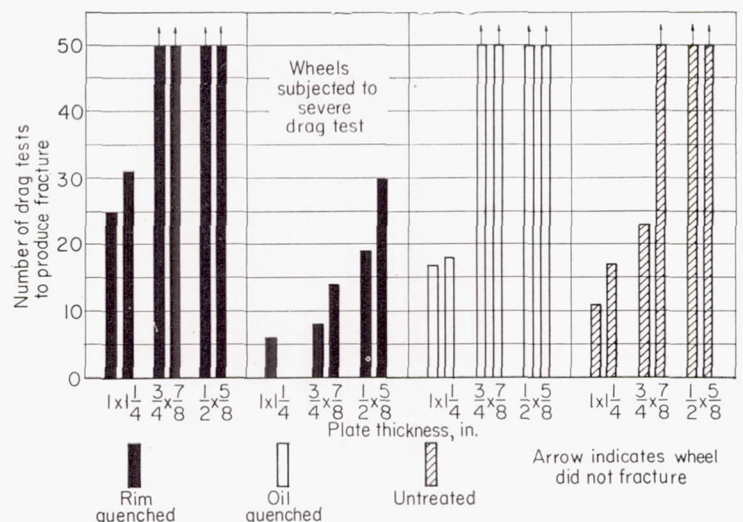


FIGURE 41.—Effect of plate thickness on number of drag tests required to produce fracture (from ref. 13).



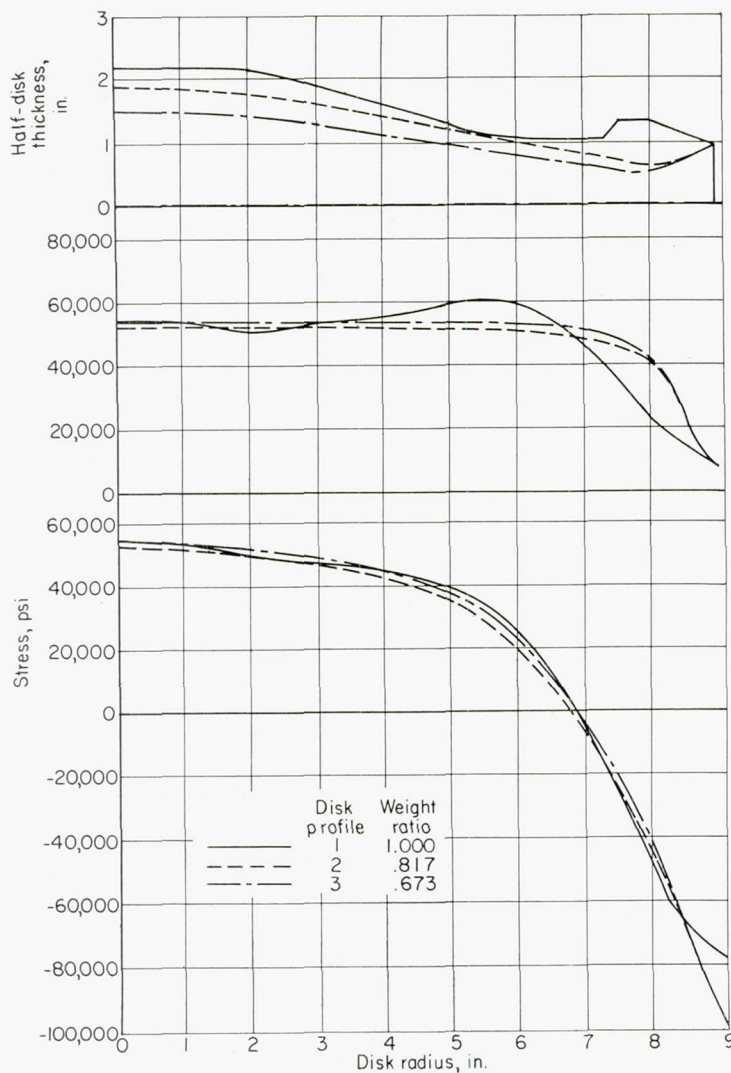


FIGURE 42.—Elastic stress distribution for various disk profiles (from ref. 11).

$\alpha_A$  is the coefficient of expansion and  $l_A$  is the length of section A, must be matched by an elongation due to stress in sections B and C. If the cross section of B is massive compared with that of C, all the strain is induced in section C. Thus, if  $\epsilon_c$  is the strain in C,

$$\epsilon_c l_c = \alpha_A T_A l_A \quad (16)$$

or

$$\epsilon_c = \frac{l_A}{l_c} \alpha_A T_A \quad (16a)$$

In the elastic range the stress induced in C as a result of this strain is

$$\sigma = E_c \epsilon_c = \frac{l_A}{l_c} E_c \alpha_A T_A \quad (17)$$

where  $E_c$  is the elastic modulus of section C.

The foregoing case illustrates the very important fact that geometrical configuration may impose a stress and strain

multiplication factor. The product  $E\alpha T_0$  is sometimes thought of as the maximum stress due to temperature change  $T_0$  that can be imposed at a point, since this product represents the stress required to constrain completely the thermal dilation. It is seen, however, from this example that the maximum stress in the system may be many times the stress for complete constraint, depending on the value  $l_A/l_c$ . Thus, unusually high stresses are frequently imposed on the weakest member of a system. If C were, for example, a weld of small axial dimension compared with sections A and B, the ratio  $l_A/l_c$  would be very large, and failure of the weld would occur at low temperature differences in the system. This failure would be due not to poor strength of the weld metal, but rather to poor design, which requires large elongations to be matched by high localized strains. In the case of welded structures, the high stresses and strains may also result if the body is at uniform temperature if the various components have different coefficients of thermal expansion. This illustration thus emphasizes one of the many reasons welds are so sensitive to thermal cycling.

#### EFFECT OF INITIAL SURFACE STRESS

In some cases it is possible to introduce initial stresses that counteract the effect of thermal stress and thereby improve thermal shock resistance. The use of shot blasting, for example, in order to introduce compressive surface stresses has been amply demonstrated in the case of mechanical fatigue at room temperature. The same idea can be applied to parts operating at high temperature provided the temperature is not so high as to anneal the induced stresses. In some cases the surface stresses should be tensile, in others, compressive; and illustrations of each will now be presented.

**Residual tension.**—In the case of turbine wheels, the operating stresses are compressive; hence, it is desirable to introduce a residual tensile stress to offset the operating stress. This can be achieved when the wheel is constructed in two parts, such as shown in figure 44. The central region, where the temperature is low, is usually made of ferritic material that can easily be forged and has good low-temperature strength. The rim region is generally made of austenitic

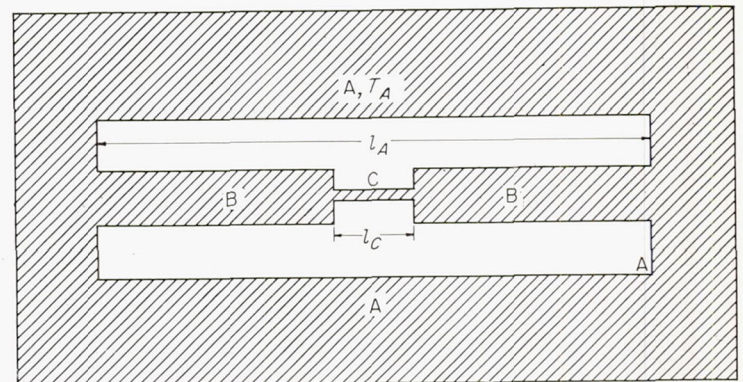


FIGURE 43.—Cross section of body in which large stress and strain are induced in small member as a result of temperature change in large member.



material which has good high-temperature strength, necessary for resisting the high temperature in this area. The two parts are joined by providing space for weld metal, as shown in the figure. One practice that has been followed is to heat the rim region to a higher temperature than the central region before insertion of the weld metal. When the rim cools, it therefore effectively shrinks onto the center region and sets up a system of residual stresses, tensile at the rim and compressive at the center. In subsequent operation the induced thermal compressive stress at the rim is counteracted by the initial tensile stress. In the lower portion of the figure is shown the stress distribution that would occur in this case if the temperature differential of  $400^{\circ}\text{F}$  were maintained between the rim and the center region during the welding procedure. This stress distribution is calculated for the disk previously discussed for which, without this shrinking practice, the compressive stress at the center would be about 60,000 pounds per square inch and at the rim, over 100,000 pounds per square inch. The only region that suffers from high stress is the region immediately adjacent to the weld. A small amount of plastic flow may take place in this region, but the temperatures in this location are lower than at the rim, and there are no geometrical stress concentrations.

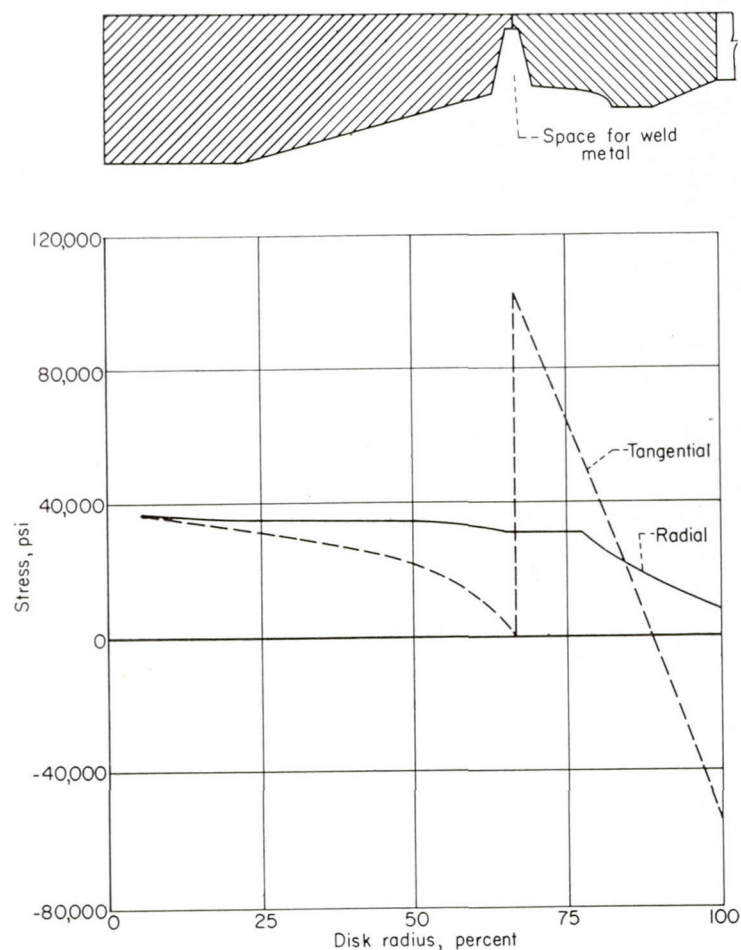


FIGURE 44.—Stress distribution in welded and shrunk disk (from ref. 11).

**Residual compression.**—In some cases the desirable initial stress is that of compression. Westbrook and Wulff (ref. 16) have, for example, made a very extensive investigation on the possibility of inducing suitable initial stresses in hollow circular cylinders. Their project was conducted in connection with the guided missile program and the interest was primarily in rocket nozzles. They therefore considered hollow cylinders that were suddenly heated in the center by a Globar rod to simulate the sudden application of combustion in the rocket nozzle. An early finding was that failure resulted first at the outer surface of the cylinder where the induced stresses were tensile. The inner surface, which heated more rapidly than the outer surface, was prevented from expanding and was thereby placed in compression, while the outer surface was forced to expand more than it would have in accordance with its temperatures and therefore was placed in tension. Although the compressive stresses in the inner surface were higher than the tensile

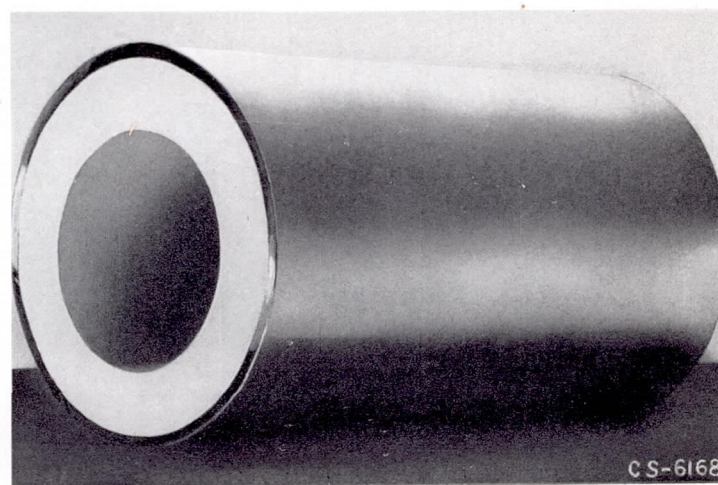


FIGURE 45.—Photograph of metal-sprayed ceramic test cylinder machined and ready for thermal shock test (from ref. 16).

stresses on the outer surface, the materials investigated were more sensitive to tensile stress than to compressive stress, and failure occurred on the outer surface. Also investigated in reference 16 was the possibility of inducing residual compressive stress at the surface by shrinking metal onto the cylinder (see fig. 45). It was realized at the outset that merely shrinking a metal cylinder onto the ceramic core by heating the cylinder and then allowing it to cool over the core would not be satisfactory. Such an application would introduce compressive stress only in the tangential direction, not in the axial direction. Since in a long cylinder the induced stress in the axial direction is equal to that in the tangential direction, failure would then occur in the axial direction. It was therefore concluded that a metal-spraying technique would be most desirable. Figure 46, taken from reference 16, shows a method of spraying. The metal to be sprayed on the cylinder is fed through the center of a spray gun, and together with this metal are fed compressed air and oxyhydrogen gas. Combustion of the air



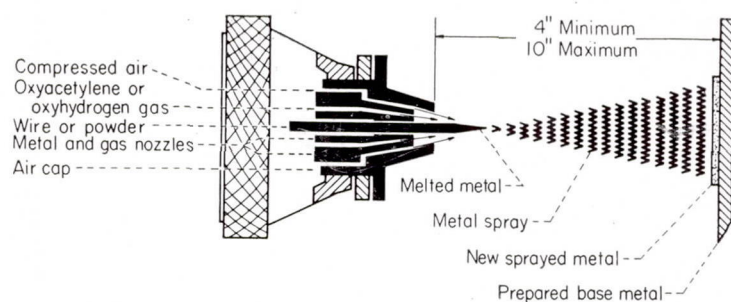


FIGURE 46.—Schematic drawing showing action of wire-type metal spray gun (from ref. 16).

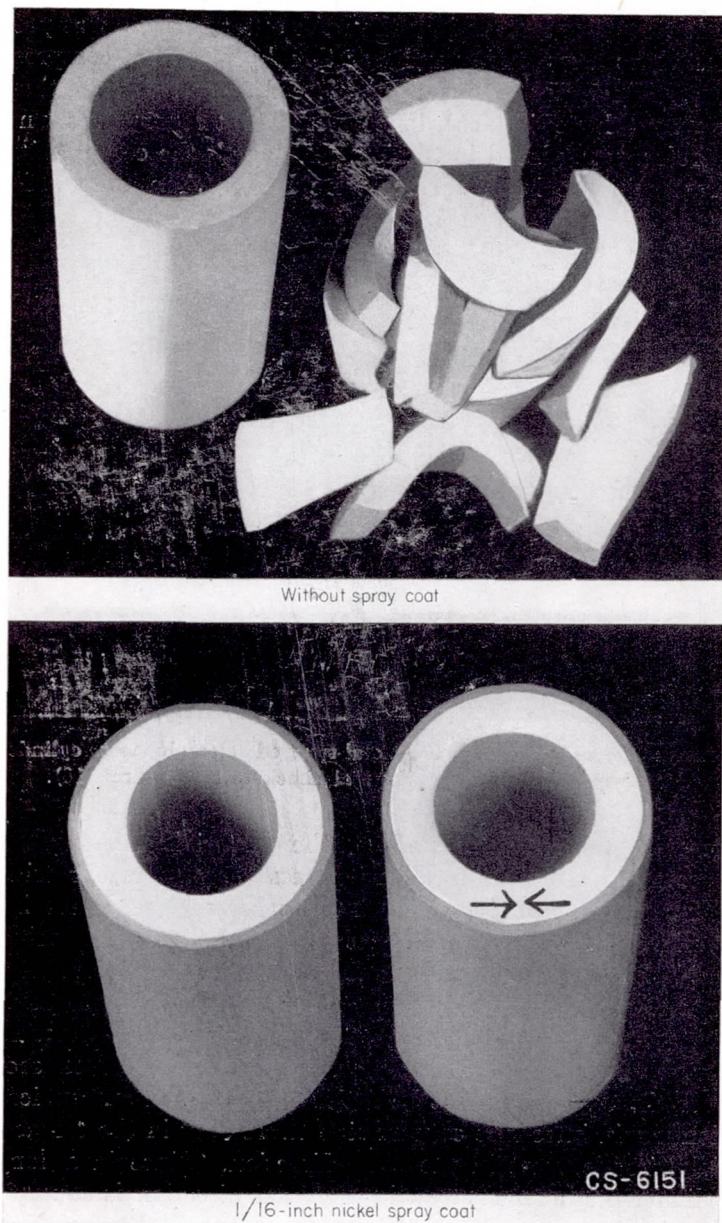


FIGURE 47.—Thermal shock tests in alumina cylinders (from ref. 16)

and fuel causes the metal to melt, and the high pressure of the fuel causes the molten metal to spray onto the cylinder. When the particles of molten metal strike the cold cylinder,

they contract in all directions and thereby induce stresses not only in the circumferential direction but also in the axial direction. In this way beneficial residual stresses are induced in the ceramic cylinder. Figure 47 demonstrates the results of their tests. The alumina cylinder metallized with  $\frac{1}{16}$ -inch nickel did not fail, while in the same test the unmetallized cylinder broke into many pieces.

Shown in figure 48, taken also from reference 16, are more complete results on the effect of metallizing on thermal shock resistance of alumina cylinders. The thermal shock resistance is plotted as a function of the ratio of metal to ceramic thickness. With molybdenum as a spray coating, all thicknesses of metal improved the thermal shock resistance, although with thickness ratios greater than one-half, the additional improvement was relatively small. For copper and stainless steel coatings of small thickness the

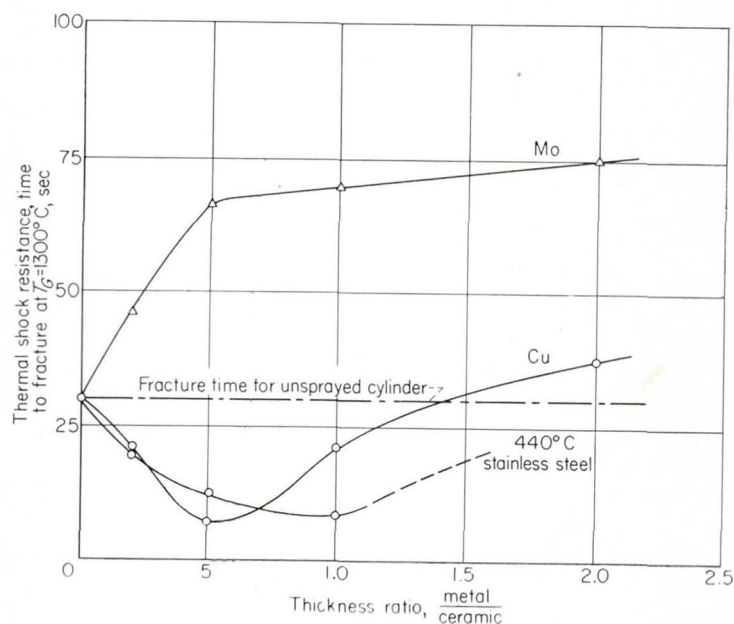


FIGURE 48.—Effect of metal/ceramic thickness ratio on thermal shock resistance of metal-sprayed cylinders (from ref. 16).

coating reduced the thermal shock resistance, but for very large thicknesses the thermal shock resistance was improved. The interaction of the coating and the ceramic under thermal shock conditions is concluded in the report to be in relatively complex relation. From the practical standpoint, it is demonstrated that improvement in thermal shock resistance can be obtained by metallizing. The possibility of inducing beneficial surface stresses by wire winding and by quenching is also discussed in reference 16, but no data are presented to substantiate the theory.

**Stress relaxation.**—It is, of course, important to emphasize that the beneficial effects of prestressing can persist only if the operating temperatures are not so high as to cause relaxation. No data are available on the subject of stress relaxation as applied particularly to the subject of thermal shock. However, important conclusions can be drawn from an in-



vestigation conducted in connection with high-temperature fatigue. A program was conducted to determine the effect of surface finish and surface working on the fatigue properties of low-carbon N-155 alloy (ref. 17). Some of the results are shown in figure 49. In the upper part of the figure are shown curves of the stress versus the number of cycles to failure at room temperature for the material in three conditions of surface treatment. The specimen with roughened surface had a greater strength than the polished and the ground specimens. While this is contrary to normal finding in fatigue tests, the improvement due to roughening was attributed to cold work induced in the surface by the roughening procedure. So much cold work was induced that the concurrent detrimental effect of irregularities in the surface was overcome, and the net effect was beneficial. Similar specimens were subsequently tested at higher temperatures and the beneficial effect of roughening was found to be reduced. At 1350° F specimens with all surface conditions had essentially the same strength as shown in the lower part of the figure. Thus, at 1350° F all the beneficial effects of working were annealed in this particular material. For further verification of this conclusion, specimens were held in the three surface conditions at 1400° F for 4 hours and were then tested at room temperature. Instead of three curves, as indicated in the upper part of figure 48, for each condition of surface treatment, only one curve was obtained; thus, it was shown that holding the material at the high temperature had removed the beneficial residual stress. From a thermal shock or thermal stress standpoint, these results are significant because they emphasize the importance of operating temperature on the effectiveness of any prestressing operation.

#### EFFECT OF SURFACE COATINGS

In addition to providing a means for inducing suitable surface stresses, surface coatings have at least two other beneficial effects in relation to thermal shock—protection from deleterious atmosphere and thermal insulation.

**Atmosphere protection.**—As previously discussed, operation at high temperatures has very detrimental effects on the metallurgy of the material. While some of these effects are inherently associated with the high temperature and cannot be avoided, others relate to the high temperature in conjunction with a detrimental atmosphere. For example, as the surface of a specimen oxidizes, the thermal shock cycles do not test the original material but the resultant surface oxide. The oxide is usually weak and brittle and the material becomes poor in thermal shock resistance. Furthermore, intergranular penetration produces effective notches at the surface. The application of a ceramic coating may retard the oxidation effect and enable the material to retain its inherent shock resistance. The National Bureau of Standards has conducted extensive research directed at finding suitable protective coatings for materials that require surface protection. For example, some of this work has been toward finding a ceramic coating for the titanium carbide plus cobalt cermet under consideration for turbine application. These cermets have good thermal shock resistance and good

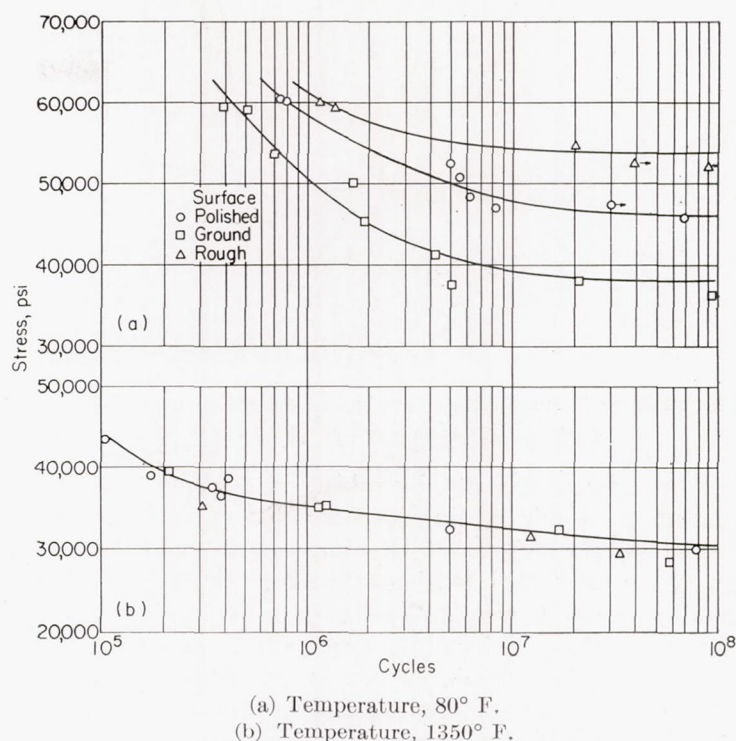


FIGURE 49.—Effect of surface treatment on fatigue properties of low-carbon N-155 (from ref. 17).

strength, but in service are attacked by oxidizing atmospheres. A coating was developed that retards the surface attack; and it was found that thermal shock resistance of coated specimens was much superior to that of uncoated specimens. A summary of some of the National Bureau of Standards' results is shown in table VI, which is taken from reference 18. The thermal shock in this case consisted in heating a cylindrical specimen for 5 minutes at a given temperature, withdrawing it from the furnace, and submerging one end to a depth of 1 inch in water at room temperature. If no failure occurred, the temperature was increased 100° and the cycle repeated. The temperature at which the first failure occurred is shown in the two columns at the right for each of the prior heat treatments. A comparison with those protected by the ceramic coating shows that heating the specimens without a coating at 1650°, 1800°, 2000°, and 2200° F for the various numbers of hours indicated had a detrimental effect on the thermal shock resistance, as indicated by the lower temperatures required to cause initial failure shown in column 3.

**Thermal insulation.**—Another beneficial effect of a surface coating is the action as an insulator which effects a reduction in heat-transfer coefficient to the test surface. As shown by equations (7) and (8), thermal shock resistance is directly proportional to the heat-transfer coefficient, except for the most drastic of quench conditions represented by very high values of  $\beta$ . In the solution of transient temperature problems, the heat-transfer coefficient is sometimes modified by substituting an equivalent film of conductive material at the surface of the test body. Thus, high heat-transfer coefficients are represented by taking very thin films, and low



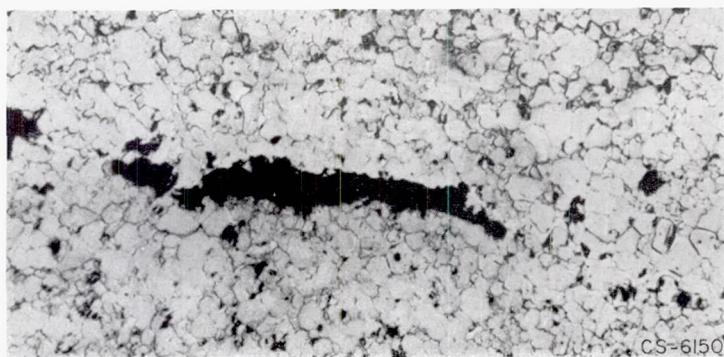


FIGURE 50.—Thermal shock crack in 11.8 weight percent (7.8 volume percent) iron plus titanium carbide cermet.

heat-transfer coefficients, by taking thick films. The presence of a ceramic coating increases the equivalent surface film thickness and makes any imposed thermal shock less severe than it would be without the film. Even if the ceramic coating cracks, it may still act as a heat-retarding medium and reduce the severity of the shock at the test surface. No analysis has been made of this insulation effect, but it is believed to be an important function of a surface coating, especially when the imposed thermal shock is of short duration.

#### EFFECT OF DUCTILITY

Ductility is one of the most important characteristics which affect the thermal shock resistance of a material. If the environmental temperature and atmosphere are not such as to destroy ductility by embrittlement, the ductile material will withstand considerably more severe thermal shocks than brittle materials of comparable tensile strength and

other mechanical and thermal properties. One of the concepts that led to the development of the metal-ceramic combinations known as cermets was the thought that the metal would impart ductility to the combination, and thereby impart good thermal shock resistance. In practice this hope has not been fully substantiated. Despite appreciable metal content, many cermets show no measurable ductility at room temperature and only very minor ductility at high temperature. But even this small ductility greatly improves the thermal shock resistance. Some evidence of ductility in the thermal shock test of a cermet is shown in figure 50. This figure was obtained in connection with the work of reference 19, although it was not published therein. The photomicrograph shows the cracks induced in a cermet of titanium carbide and iron. The large dark areas are the cracks, and in between these cracks are areas of continuous metal phase that are apparently elongated; that is, the width of the metal band is much greater in this area than in other areas of the photograph. The evidence of ductility given here is only slight, and perhaps inconclusive, but it is believed that cermets do show some ductility in thermal shock tests at high temperature.

#### EFFECT OF CONDUCTIVITY

The significance of conductivity on thermal shock resistance of brittle materials has already been discussed in the first part of this report. Although, under very unusual circumstances, high conductivity may be undesirable, the usual case is that good conductivity improves thermal shock resistance. Not only does good conductivity generally reduce stresses during the thermal shock process, but it frequently reduces working temperatures and hence brings many metals into an operating temperature range where their strength is greater. Haythorne (ref. 20) rates conductivity as one of the most important properties in high-temperature applications of sheet metal. In these tests, tubes 2 inches in diameter and 5 inches in length were subjected to a gas flame impingement  $1\frac{1}{2}$  inches from one end. It was demonstrated first that operating temperatures bear an inverse relation to conductivity. Some of the results of reference 20 are shown in figure 51. Here the temperature distribution along the length of the tube is plotted for several different materials. The high-temperature materials, which have poor conductivities, are seen to operate with a peak temperature in the neighborhood of  $2000^{\circ}\text{F}$  and a minimum temperature of  $550^{\circ}\text{F}$  at the far end of the tube. A good conductor, such as copper, shows a maximum temperature of  $1530^{\circ}\text{F}$  and no other temperature below  $1100^{\circ}\text{F}$ . Copper does not, of course, have the strength or corrosion resistance to withstand operating conditions. The desirable characteristics of both the high-temperature materials and the good conductors are combined in a clad material. Figure 52 shows the test results. The number of test cycles which the Inconel-clad copper sheet withstood compared with the other materials is very striking.

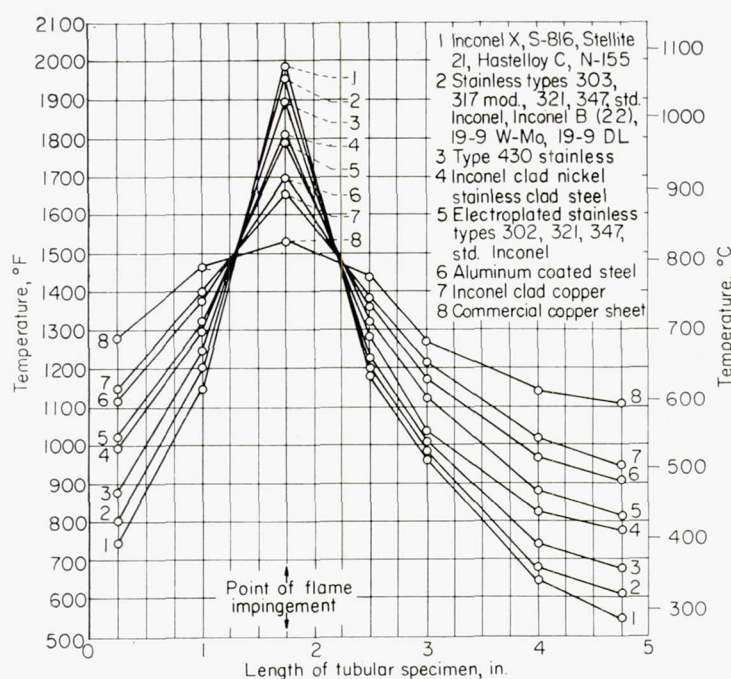


FIGURE 51.—Operating temperatures (from ref. 20).



Cermets, too, owe part of their superior thermal shock resistance to high conductivity. Although in the case of titanium carbide cermets the conductivity is not much better than that of the titanium carbide itself, many cermets involve the use of ceramics of poor conductivity and the metal additions help greatly to improve the conductivity and thermal shock resistance.

#### EFFECT OF COEFFICIENT OF EXPANSION

In brittle materials thermal shock resistance is inversely proportional to coefficient of expansion in all ranges of the nondimensional heat-transfer index  $\beta$ . Hence, any reduction that can be made in expansion coefficient will effect a proportional increase in thermal shock resistance. Even in ductile materials, the coefficient of expansion is of major importance. Obviously, in the extreme, if the coefficient of expansion is zero there will be no thermal stress. Materials of low coefficient of expansion involve low thermal strain and stress, and therefore should, everything else being equal, be superior in thermal shock resistance to materials of high coefficient of expansion.

For brittle materials, considerable use has been made of the concept of reducing coefficient of expansion to gain in thermal shock resistance. Pyrex, a silica glass, owes its

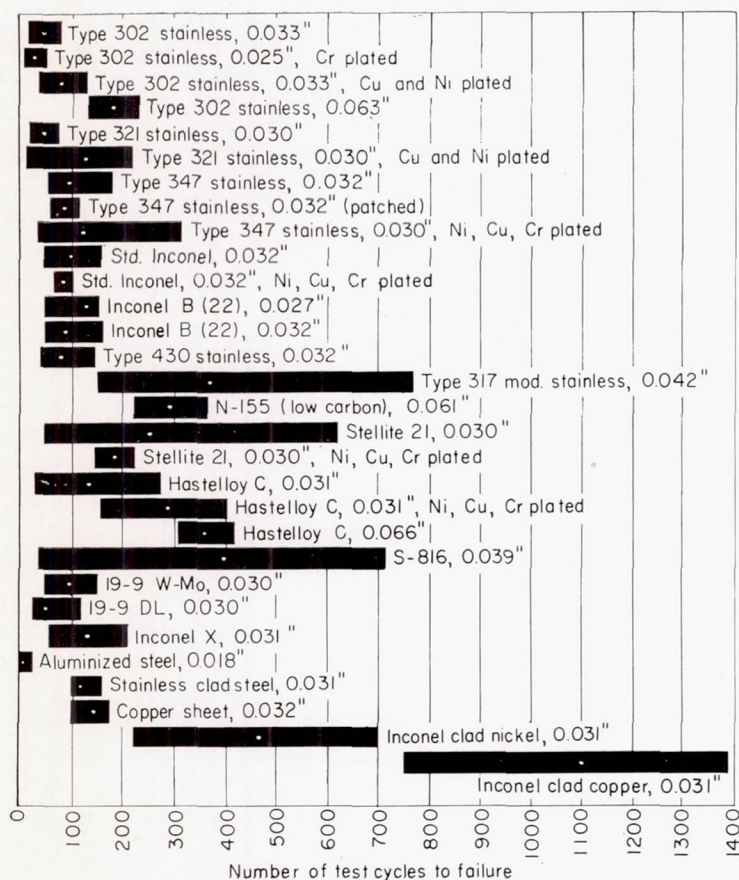


FIGURE 52.—Summarized results of flame impingement test (from ref. 20).

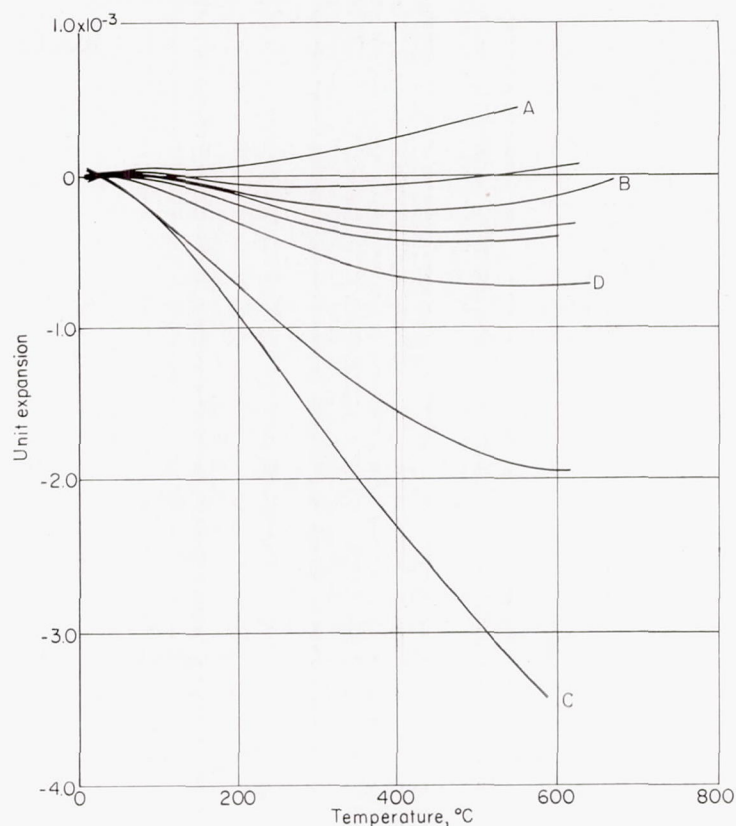


FIGURE 53.—Typical thermal expansion curves of various Stupalith compositions (from ref. 21).

outstanding thermal shock resistance to its very low coefficient of expansion. Unfortunately, it is poor in creep resistance and therefore does not lend itself especially well to applications involving prolonged stress at high temperature.

Recently there has been developed a new series of ceramics known as Stupalith. These ceramics are produced from blends of lithium-bearing materials and clay, or blends of other ceramic raw materials to obtain the desired ratio of lithia, alumina, and silica. By variations in composition, the coefficient of expansion can be controlled over a wide range and can even be made negative. The main advantage lies in the fact that it can be made close to zero. Figure 53 (ref. 21) shows typical expansion curves for various Stupalith compositions. Material A has a positive, but low coefficient of expansion; the coefficient of expansion of material B is very close to zero; while materials C to D have negative coefficients of expansion, that is, they contract upon heating. The zero-expansion material is said to have outstanding thermal shock resistance. The manufacturers test their materials by heating specimens to 2000° F and then dropping them into liquid air at -310° F. It is claimed that this procedure can be repeated 100 times without ill effect. The geometry of the specimen is not disclosed, but it is presumed that the type of test is severe stresswise. They suggest the use of these materials for turbine blades, nozzle inserts, and other jet and internal combustion engine parts.



## EFFECT OF ELASTIC MODULUS

In the case of brittle materials, thermal shock resistance is inversely proportional to elastic modulus. Hence, low elastic modulus is an asset to good thermal shock resistance. Graphite, for example, owes its good thermal shock resistance, at least in part, to its very low elastic modulus, approximately  $0.7 \times 10^6$  pounds per square inch. While the major attribute of pyrex glass is its low thermal coefficient of expansion, it should be noted that its outstanding over-all characteristic is due also to its relatively low elastic modulus, approximately  $8.5 \times 10^6$  pounds per square inch.

Cermets, and some of the other newer materials under development, are characterized by extremely high elastic modulus. For example, the elastic modulus of an 80 percent titanium carbide plus 20 percent cobalt cermet is  $60 \times 10^6$  pounds per square inch, twice that of steel. Were it not for the outstanding conductivity, strength, and possibly ductility, this large elastic modulus would be a great drawback in its thermal shock resistance.

In ductile materials the elastic modulus is probably also important, but not so much as in brittle materials. Bentele and Lowthian (ref. 9), in summarizing the German nozzle vane tests, state that the number of cycles to failure was inversely proportional to the one-third power of elastic modulus, although the relation was valid only in a limited range of number of cycles to failure. In any case, thermal shock resistance bears an inverse relation to elastic modulus, all other factors being equal.

## JOINING OF DISSIMILAR METALS

The problem of thermal stress and thermal shock is one of extreme importance in the field of welding. Here, dissimilar metals are joined together, these dissimilar metals being either parts welded together or the weld metal. Differential thermal expansion between the different metals, cracks initiated during the welding, friction oxidation between the welded parts, and metallurgical interaction between the dissimilar materials all contribute to loss of thermal shock resistance. This subject is very extensively discussed in a recent survey by the Welding Research Council (ref. 22).

## CONCLUDING REMARKS

The important points that have been indicated in connection with the behavior of materials under thermal stress conditions may be summarized as follows:

1. It has been emphasized that the best measure of thermal shock resistance in brittle materials is the determination of a temperature difference that will cause failure in one cycle. Not only does this procedure render the problem tractable to analysis without introducing the complications of thermal fatigue, but the experimental results for the single-cycle type of test are usually reproducible and contain a minimum of scatter. It is recognized, however, that the practical consideration really involves the number of cycles of a given nature that a specimen can withstand without failure. Hence tests of both the single-cycle and multiple-cycle failure may be necessary before a valid comparison can be made among materials.

2. Simple formulas have been presented for thermal shock resistance by the single-cycle criterion. These formulas involve both indices now recognized in the literature,  $k\sigma_b/E\alpha$  and  $\sigma_b/E\alpha$ . Neither index can, therefore, by itself provide a basis for rating materials under all test conditions. Most practical cases fall, however, in the range where  $k\sigma_b/E\alpha$  is the primary index for rating brittle materials. It is only under the most severe of shock conditions that the  $\sigma_b/E\alpha$  index predominates; in general, therefore, this index usually merely modifies the  $k\sigma_b/E\alpha$  index. Hence, in most cases thermal shock can be improved by increases in conductivity. It should also be emphasized that the formulas apply only to the infinite flat plate, but similar formulas could probably be derived by the same method for other cases involving one-dimensional heat transfer. Likewise, it should be emphasized that the formulas are applicable only when the duration of the shock is long enough to permit the maximum stress to be developed. There are practical cases when shock duration is low, and therefore other criteria may prevail. In the case of rocket nozzles, for example, it might be advantageous to use materials of low conductivity rather than the better conductors. Each case requires a separate analysis.

3. It is important to test the materials under conditions not far different from the intended test application; otherwise, relative merits of materials may interchange and experimental results may give erroneous predictions.

4. It has been emphasized that for ductile materials the single-cycle criterion is not practical because it is rare that failure can be achieved in one cycle. The use of the multiple-cycle criterion further complicates the already complex problem which involves metallurgical processes occurring during and in between thermal shock cycles. Some of these processes have been discussed and their potential relation to thermal shock resistance indicated. In view of the importance of metallurgical processes, and of the importance of temperature influence on action of metallurgical processes, the danger of conducting tests under artificial conditions becomes strikingly evident. Increasing temperatures in order to accelerate failure may introduce spurious metallurgical effects, foreign to the behavior of the materials under their true working conditions. Hence it is very important that the tests simulate the operating conditions irrespective of whether this entails a larger number of tests before failure occurs.

5. A number of important variables have been outlined which can actually assist in producing designs of improved thermal shock resistance. Among these, emphasis has been placed on the reduction of stress concentrations and constraints and the introduction of favorable initial stress and surface protection. Control may also be exercised over the metallurgical variables, but first much research toward understanding them is necessary.

LEWIS FLIGHT PROPULSION LABORATORY  
NATIONAL ADVISORY COMMITTEE FOR AERONAUTICS  
CLEVELAND, OHIO, December 19, 1952



## REFERENCES

- Bradshaw, F. J.: Thermal Stresses in Non-Ductile High Temperature Materials. Tech. Note MET. 100, British R. A. E., Feb. 1949.
- Cheng, C. M.: Resistance to Thermal Shock. Jour. Am. Rocket Soc., vol. 21, no. 6, Nov. 1951, pp. 147-153.
- Buessem, Wilhelm: The Ring Test and Its Application to Thermal Shock Problems. Metallurgy Group, Office Air Res., Wright-Patterson Air Force Base, Dayton (Ohio), June 1950.
- Bobrowsky, A. R.: The Applicability of Ceramics and Ceramals as Turbine Blade Materials for the Newer Aircraft Power Plants. Trans. A. S. M. E., vol. 71, no. 6, Aug. 1949, pp. 621-629.
- Bradshaw, F. J.: The Improvement of Ceramics for Use in Heat Engines. Tech. Note MET. 111, British R. A. E., Oct. 1949.
- Liu, S. I., Lynch, J. J., Ripling, E. J., and Sachs, G.: Low Cycle Fatigue of the Aluminum Alloy 24ST in Direct Stress. Tech. Pub. No. 2338, Am. Inst. Mining and Metallurgical Eng., Feb. 1948.
- Sachs, George, and Brown, W. F., Jr.: A Survey of Embrittlement and Notch Sensitivity of Heat Resisting Steels. A. S. T. M. Spec. Tech. Pub. No. 128, 1952.
- Rush, A. I., Freeman, J. W., and White, A. E.: Abnormal Grain Growth in S-816 Alloy. NACA TN 2678, 1952.
- Bentele, M., and Lowthian, C. S.: Thermal Shock Tests on Gas Turbine Materials. Aircraft Eng., vol. XXIV, no. 276, Feb. 1952, pp. 32-38.
- Whitman, M. J., Hall, R. W., and Yaker, C.: Resistance of Six Cast High-Temperature Alloys to Cracking Caused by Thermal Shock. NACA TN 2037, 1950.
- Manson, S. S.: Stress Investigations in Gas Turbine Discs and Blades. SAE Quarterly Trans., vol. 3, no. 2, Apr. 1949, pp. 229-239.
- Wilterdink, P. I., Holms, A. G., and Manson, S. S.: A Theoretical and Experimental Investigation of the Influence of Temperature Gradients on the Deformation and Burst Speeds of Rotating Disks. NACA TN 2803, 1952.
- Wetenkamp, Harry R., Sidebottom, Omar M., and Schrader, Herman J.: The Effect of Brake Shoe Action on Thermal Cracking and on Failure of Wrought Steel Railway Car Wheels. Bull. 387, Eng. Exp. Station, Univ. of Illinois, vol. 47, no. 77, June 1950.
- Wilterdink, P. I.: Experimental Investigation of Rim Cracking in Disks Subjected to High Temperature Gradients. NACA RM E9F16, 1949.
- Weeton, John W.: Mechanisms of Failure of High Nickel-Alloy Turbojet Combustion Liners. NACA TN 1938, 1949.
- Westbrook, J. H., and Wulff, J.: The Thermal Shock Resistance of Metallized Hollow Ceramic Cylinders. Meteor Rep. No. 44, M. I. T., 1949.
- Ferguson, Robert R.: Effect of Surface Finish on Fatigue Properties at Elevated Temperatures. I—Low-Carbon N-155 with Grain Size of A. S. T. M. 1. NACA RM E51D17, 1951.
- Moore, Dwight G., Benner, Stanley G., and Harrison, William N.: Studies of High-Temperature Protection of a Titanium-Carbide Ceramal by Chromium-Type Ceramic-Metal Coatings. NACA TN 2386, 1951.
- Cooper, A. L., and Colteryahn, L. E.: Elevated Temperature Properties of Titanium Carbide Base Ceramals Containing Nickel or Iron. NACA RM E51I10, 1951.
- Haythorne, P. A.: Sheet Metals for High Temperature Service. Iron Age, vol. 162, no. 13, Sept. 23, 1948, pp. 89-95.

TABLE I.—CORRELATION OF MATERIAL PROPERTIES WITH RESISTANCE TO FRACTURE BY THERMAL SHOCK

Order of merit of materials evaluated in thermal shock	Thermal shock cycles before failure				Coefficient of thermal expansion, $\alpha$ , in./in./°F	Thermal conductivity, $K$ , Btu/in./hr/sq ft/°F	Effective modulus of elasticity at 1800° F, $E$ , lb/sq in.	Tensile strength at 1800° F, $S$ , lb/sq in.	$\frac{KS}{\alpha E}$
	Temperature, °F								
	1800	2000	2200	2400					
Alloy A	(a)				$8.24 \times 10^{-6}$	140	$0.10 \times 10^7$	33,300	566,000
80 percent TiC+20 percent Co	25	25	25	b 25	5.5	240	6.0	34,600	25,200
TiC	25	25	25	17	4.56	c 240	c 6.0	17,200	15,100
BeO	25	3			5.1	104	4.28	6,200	2,950
ZrSiO <sub>4</sub>	1				2.51	11.6	2.4	8,700	1,700
MgO	$\frac{1}{2}$				7.69	16-40	1.24	3,100	520-1300
94 percent ZrO <sub>2</sub> +6 percent CaO	0				d 5.53	d 14.3	d 2.5	6,750	700

<sup>a</sup> Not yet evaluated, but probably best of all materials given.<sup>b</sup> No failure.<sup>c</sup> Value for 80 percent TiC+20 percent Co.<sup>d</sup> Value for ZrO<sub>2</sub>.

TABLE II.—RELATIVE REDUCTION OF THERMAL SHOCK CYCLES WITH INCREASE IN TEMPERATURE

$$\left[ \frac{N_2}{N_1} = \left( \frac{\alpha T_1 - 2e_y}{\alpha T_2 - 2e_y} \right)^3 \right]$$

Evaluation temperature, °F	Relative reduction of thermal shock cycles at comparison temperature of—			
	1000° F	1200° F	1400° F	1600° F
1000	1.0	-----	-----	-----
1200	4.7	1.0	-----	-----
1400	12.6	2.8	1.0	-----
1600	27	5.8	2.1	1.0
1800	49	9.7	3.9	1.6

TABLE IV.—RELATION BETWEEN THERMAL SHOCK RESISTANCE AND IMPACT STRENGTH

Alloy	S-816	S-590	Stellite 21	422-19	X-40	Stellite 6
Cycles to failure .....	$\left\{ \begin{array}{l} 86 \\ 104 \\ 105 \end{array} \right.$	$\left\{ \begin{array}{l} 34 \\ 34 \\ 36 \end{array} \right.$	$\left\{ \begin{array}{l} 24 \\ 30 \end{array} \right.$	$\left\{ \begin{array}{l} 6 \\ 6 \end{array} \right.$	$\left\{ \begin{array}{l} 7,6 \\ 7,7 \end{array} \right.$	$\left\{ \begin{array}{l} 2,12,4 \\ 2,2,2 \end{array} \right.$
Charpy V-notch impact strength at 70° F (ft-lb) .....	4.7	3.2	2.9	1.5	2.3	2.4

TABLE III.—THERMAL SHOCK TESTS IN NOZZLE BLADES

No.	Material	N <sub>1</sub> *		N <sub>2</sub> **	
		(T).	A.	B.	
1	W. F. 100 D .....	834	-----	-----	360
2	DVL 30 .....	1645	-----	-----	56
5	DVL 3 3/4 .....	1130	60	-----	137
9	SAS 8 .....	858	-----	-----	-----
10	ATS .....	1023	40	-----	-----
14	W. F. 200 .....	1800	-----	-----	364
18	P. 193 .....	1393	-----	-----	83
19	B. 7M .....	1050	-----	-----	94
21	DVL 32 .....	1280	-----	-----	44

\*N<sub>1</sub>. Number of cycles at 650-700° C before the onset of distortion or cracking.\*\*N<sub>2</sub>. Number of cycles at 850-900° C before the onset of:

(a) Distortion.

(b) Cracking.



TABLE V.—EFFECTS OF REAMING, SANDING, AND VAPOR BLASTING OF PUNCHED EDGES ON CRACKING OF COMBUSTION-CHAMBER LINERS

Time in accelerated life runs		Average number of cracks in seven as-fabricated liners	Average number of cracks in seven reamed, sanded, and vapor-blasted liners
hr	min		
8	20	8.43	1.86
16	40	20.29	9

TABLE VI.—EFFECT OF CERAMIC COATING ON THERMAL SHOCK RESISTANCE OF CERMET

Treatment before thermal shock		Temperature of 1st failure with no coating, °F	Temperature of 1st failure of coating (2 coats), °F
Time, hr	Temperature, °F		
400	1650	1300	>2200
200	1800	1200	>2200
100	2000	1500	>2200
50	2200	1600	2200